Parallel Session 10

Structure Functions and Deep Inelastic Scattering



Organisers

A. W. Thomas (Adelaide)
M. Klein (IFP, Zeuthen)

NMC Results from F₂ Structure Functions

JAN NASSALSKI * NIKHEF-K, P.O.Box 4395, 1009 AJ Amsterdam. The Netherlands.

Abstract

Preliminary results on $F_2^p(\mathbf{x}) - F_2^n(\mathbf{x})$ and on $F_2^n/F_2^p(\mathbf{x},Q^2)$ obtained with a 90GeV and 280GeV muon beam, on the x-dependence of F_2^{Ca}/F_2^d and F_2^C/F_2^d at 200GeV and on F_2^{Ca}/F_2^C at 90GeV are presented. The difference $F_2^p - F_2^n$ indicates a deviation from the Gottfried sum rule. The ratio F_2^n/F_2^p shows a stronger Q^2 -dependence than the one predicted from NLO QCD with TM corrections. The ratio F_2^{Ca}/F_2^C is below unity for $\mathbf{x} \leq 0.1$, exhibiting stronger shadowing in Ca, while it does not exceed unity for the larger \mathbf{x} .

1 Introduction.

The New Muon Collaboration (NMC) has performed measurements of deep inelastic muon scattering on several target materials which were simultanously exposed to the beam. The measurements covered a kinematic range down to x=0.0035 and $Q^2=0.5 \, \mathrm{GeV}^2$.

The x-distributions are discussed in terms of the Quark-Parton Model; the flavour symmetry of the nucleon sea and the momentum sum of the charged partons in the nucleus. The Q^2 -dependence of the ratio F_2^n/F_2^p is used to extract the difference of higher twist terms in scattering on hydrogen and deuterium targets.

2 The Gottfried Sum Rule.

In the Quark-Parton Model (QPM), assuming isospin symmetry between the proton and the neutron, the integral $S_G \equiv \int_0^1 (dx/x) \cdot (F_2^p - F_2^n)$ can be writted as a sum of two terms:

$$S_G = 1/3 \int_0^1 dx (u_v - d_v) - 2/3 \int_0^1 dx (\bar{d} - \bar{u}),$$
 (1)

where $u_v(\bar{u})$ and $d_v(\bar{d})$ are valence(sea) parton distribution functions in the proton.

In the QPM, the value of the first integral is unity. If the sea is flavour symmetric $(\bar{d} = \bar{u})$ then $S_G=1/3$. QCD corrections to this result are known to be small [1]. Therefore a deviation from 1/3 can be interpreted as the signature of a flavour symmetry breaking in the sea.

*On leave of absence from the Soltan Institute for Nuclear Studies, Warsaw. Present address: CERN, EP Division, CH-1211 Geneva 23. Previous experimental results come from the EMC [2] and the BCDMS collaboration [3], and both were found to be consistent with $S_G=1/3$ within the errors. In these experiments one of the main sources of uncertainties was the large contribution to S_G from the extrapolation of $F_2^p - F_2^n$ to the unmeasured region:

Expt.	$\triangle x_{meas}$.	$(S_G)_{meas}$.	$(S_G)_{unmeas}$.
EMC	0.02 - 0.8	$0.197 \pm 0.011 \pm 0.083$	0.038
BCDMS	0.06 - 0.8	$0.197 \pm 0.006 \pm 0.036$	0.07 - 0.22

where $(S_G)_{meas.}$ is the value of the integral (1) over the measured region of x $(\triangle x_{meas.})$.

The preliminary results from the NMC measurements extend down to x = 0.004 and the uncertainty in the extrapolation is therefore reduced. Fig.1 shows preliminary results on $F_2^p(\bar{x}) - F_2^n(\bar{x})$ at $Q^2 = 4 \text{GeV}^2$ together with the values of the in-

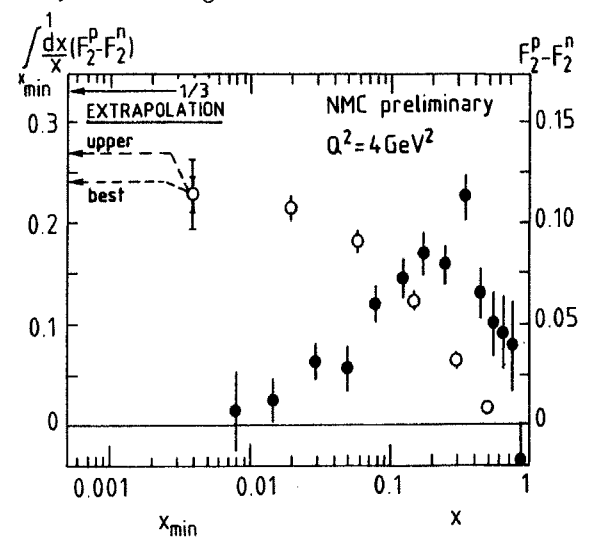


Figure 1: $F_2^p(\bar{\mathbf{x}}) - F_2^n(\bar{\mathbf{x}})$, full symbols and the scale on the right, and $S_G(x_{min.})$, open symbols and the scale on the left, from the NMC 280 GeV data.

tegral $S_G(x_{min}) \equiv \int_{x_{min}}^1 (dx/x) \cdot (F_2^p - F_2^n)$ obtained from the 280GeV data.

In the unmeasured region x < 0.004, $F_2^p(\bar{\mathbf{x}}) - F_2^n(\bar{\mathbf{x}})$ was assumed to vary as x^β and $\beta \simeq 0.5$ has been found to fit the points at small \mathbf{x} . The minimum value of β compatible with the data is about 0.3. The result based on the 280GeV and a small fraction of the 90GeV data is:

$$S_G(x_{min} = 0.004) = 0.230 \pm 0.013(stat.) \pm 0.027(syst.)$$
 (2)

with

$$S_G(x < x_{min}) = 0.012 - 0.040. \tag{3}$$

An alternative but not independent result has been obtained by the NMC [5] from $F_2^p - F_2^n$ defined as $F_2^p - F_2^n \equiv 2F_2^d \cdot (1-R)/(1+R)$ where $R \equiv F_2^n/F_2^p$ has been determined from 280GeV NMC data [4] and F_2^d was obtained from the fit to all muon and electron scattering data published before 1989.

The result, at
$$Q^2=15 {
m GeV^2}$$
, was: $S_G(x_{min}=0.004)=0.219\pm0.008(stat.)\pm0.021(syst.)$ and $S_G(x< x_{min})=0.010-0.020$.

Thus the NMC results consistently indicate that $S_G < 1/3$. Using the values given by (2) and (3) one obtains:

$$\int_0^1 dx (\bar{d} - \bar{u}) = 0.14 \pm 0.06. \tag{4}$$

3 The $F_2^n/F_2^p(x,Q^2)$ ratio.

The $F_2^n/F_2^p(x,Q^2)$ ratio has been determined from 90 and 280GeV muon interactions with H_2 and D_2 targets. The $\log(Q^2)$ -dependence of the ratio together with the results of a fit to a straight line in different bins of x is shown in Fig.2.

The slopes $d(F_2^n/F_2^p)/d(\ln Q^2)$ of the fitted lines for each x-bin are plotted Fig.3.

The curves show predictions from the next-to-leading order (NLO) QCD and also from NLO QCD with target mass (TM) effects [7]. In the region $0.1 \le x \le 0.3$ the data show a stronger Q^2 -dependence than the predictions. A similar trend was seen in slopes obtained from merged SLAC and BCDMS F_2^n/F_2^p data [6], however this result also depends on the relative normalisation of the two experiments.

It has been assumed that the difference in slopes between the data and the prediction from NLO QCD with the TM effects is due to other remain-

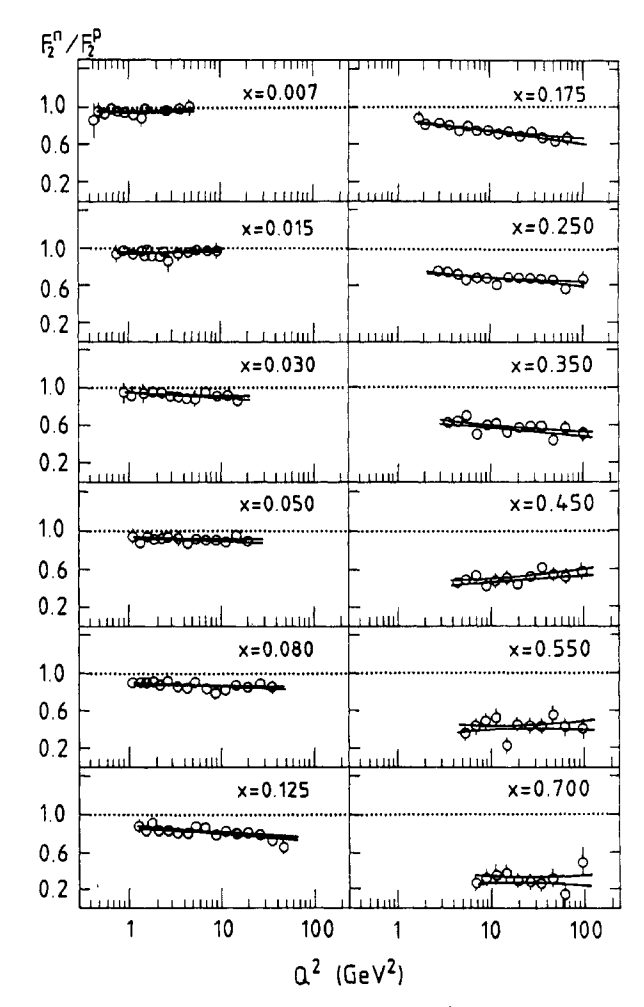


Figure 2: F_2^n/F_2^p as a function of $\log(Q^2)$ in different bins of x from the NMC data at 90 and 280GeV. The lines show error boundaries for fits to a straight line.

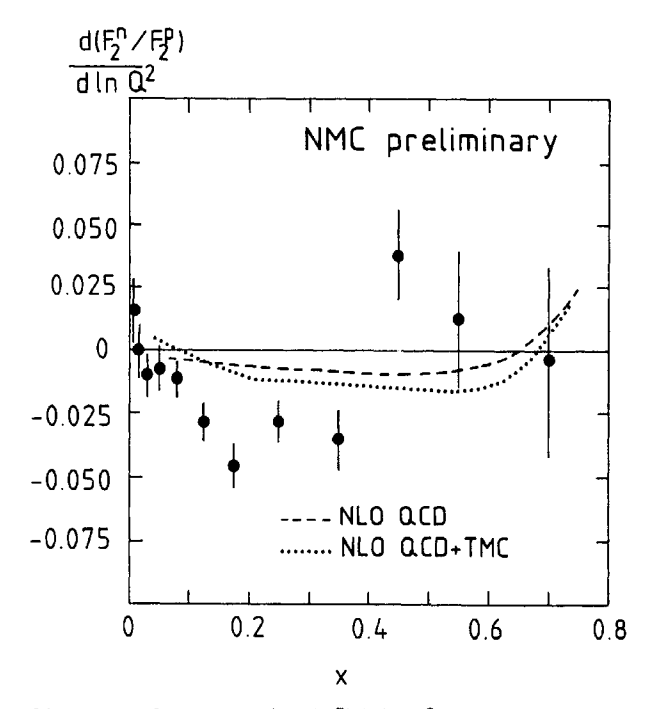


Figure 3: The slopes $d(F_2^n/F_2^p)/d(\ln Q^2)$ of the best-fitted lines in Fig.2 compared to predictions from NLO QCD (see text).

ing higher twist terms which therefore must be different for hydrogen and deuterium target. To estimate their size, the following parameterisation has been used:

$$F_{2_{meas.}}^{p(d)} = F_{2_{NLO,QCD+TM}}^{p(d)} \cdot \frac{(1 + C^{p(d)})}{Q^2}, \quad (5)$$

where $C^{p(d)}$ are the coefficients of higher twist terms for the proton (deuterium) target. This parameterisation leads to:

$$rac{dR_{meas.}}{d(lnQ^2)} \simeq rac{dR_{NLO.QCD+TM}}{d(lnQ^2)} + (1+R) \cdot rac{\left(C^p - C^d
ight)}{Q^2},$$
 (6)

where $R \equiv F_2^n/F_2^p$.

Using the calculated slopes $dR_{NLO,QCD+TM}/d(lnQ^2)$, the values for C^p-C^d have been obtained from a fit of eq.(6) to the data points shown in Fig.2. The fits had probabilities comparable to straight-line fits discussed previously. The result of the fit is shown in Fig.4.

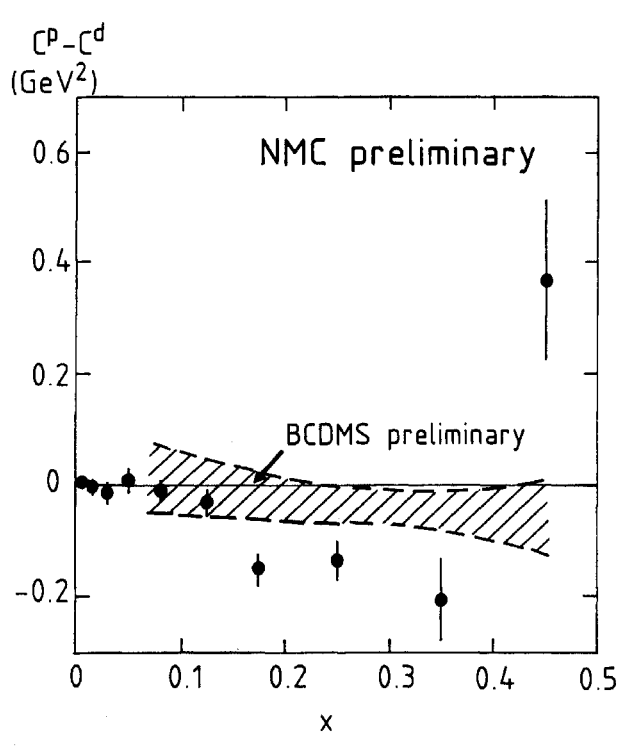


Figure 4: The difference of higher twist terms for H and D obtained from the NMC data on $F_2^n/F_2^p(\mathbf{x},Q^2)$ compared to the corresponding result obtained from F_2^p and F_2^d for SLAC+BCDMS data [8] (see text).

The shaded area in the figure shows the difference of C^p and C^d , where C^p and C^d were obtained separately from the fits of the absolute F_2^p or F_2^d , using parameterisation (5), to the SLAC and BCDMS data simultaneously [8]. The present preliminary results indicate a larger difference be-

tween higher twist terms in the F_2 structure functions for hydrogen and deuterium.

4 Ratios of F_2 from Ca/d, C/d and Ca/C targets.

Figure 5 shows the ratios $F_2^{Ca}/F_2^d(x)$ and $F_2^C/F_2^d(x)$ from 200GeV data. The average Q^2 changes from 0.6GeV^2 at x=0.0035 to 16GeV^2 at x=0.2.

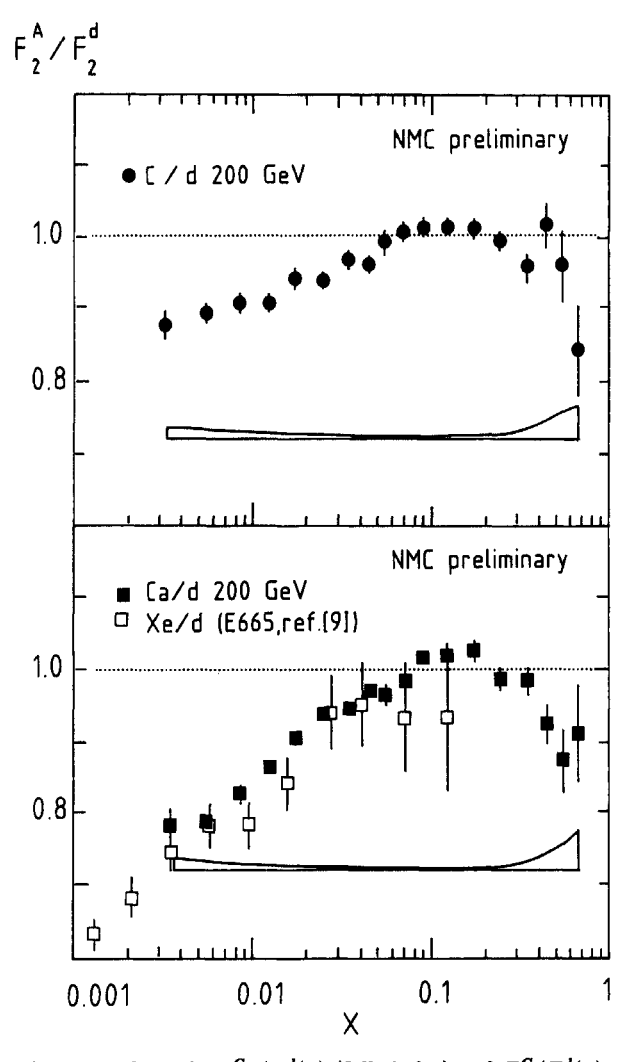


Figure 5: The ratio $F_2^{Ca}/F_2^d(x)$ (full circles) and $F_2^C/F_2^d(x)$ (full squares) from the NMC 200GeV data. The open squares show preliminary results on $F_2^{Xe}/F_2^d(x)$ from FNAL [9].

A clear shadowing signal is seen for $x \le 0.07$ and it is strongest for Ca. For 0.07 < x < 0.2 the ratio Ca/d is significantly above unity while for C/d this enhancement is less conclusive. In the same figure the preliminary results on the Xe/d ratio from the FNAL experiment E665 [9] are plotted. Within the large (8%) systematic error from this experiment, no difference in the shadowing region is seen between Xe (A=131) and Ca (A=40).

Figure 6 shows the ratio $F_2^{Ca}/F_2^C(x)$ from a higher statistics experiment at 90GeV, where the average Q^2 changes from 0.8GeV^2 at x=0.009 to 7GeV^2 at x=0.2.

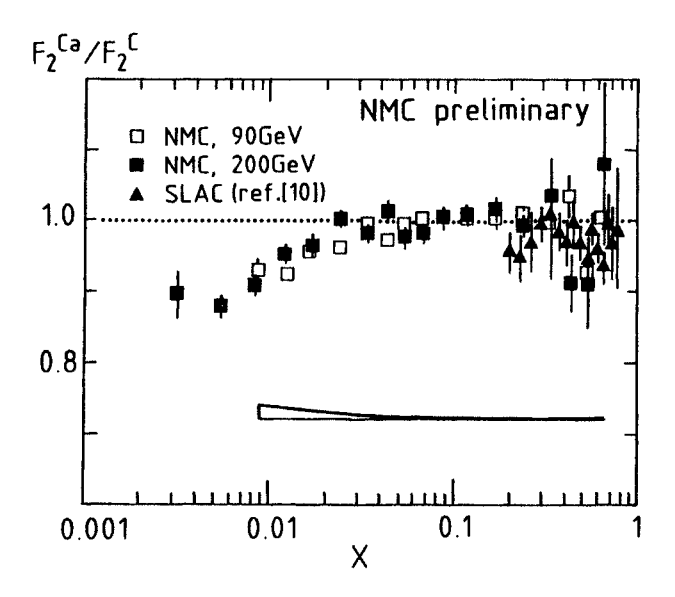


Figure 6: The ratio $F_2^{Ca}/F_2^C(x)$ from the NMC 90GeV (circles) and 200GeV (squares) data. The triangles show the same ratio from SLAC experiment [10].

Both nuclei are isoscalar and they have comparable density while the radius of Ca is 40% larger. Difference in shadowing between Ca and C is clearly seen. Outside the shadowing region the ratio is consistent with unity. This result is confirmed by a previously discussed smaller statistics experiment at 200 GeV. The ratio obtained from the SLAC experiment [10] which covered x > 0.2, also does not exceed unity. From these observations it is concluded that the integral of the structure function

$$\int dx \cdot x \cdot \sum_{i} e_{i}^{2} \cdot q_{i}(x) \tag{7}$$

of a nucleon in Ca is smaller than the one in C for the x-range covered by the measurements. In terms of the Quark-Parton Model it implies that the momentum fraction carried by all charged partons in Ca is smaller than that in C.

References

- [1] D.A.Ross and C.T.Sachrajda, Nucl. Phys. B149(1979)497.
- [2] EMC: J.J.Aubert et al., Nucl. Phys. B293(1987)740.

- [3] BCDMS: A.C.Benvenutti et al., Phys.Lett.237(1990)599.
- [4] NMC: D.Allasia et al., CERN-PPE/90-130 (1990); submitted to Phys.Lett..
- [5] NMC: presented by M. van der Heijden at Rencontres de Moriond, Les Arcs, March 1990.
- [6] L.W.Whitlow, Ph.D. Thesis, SLAC, 1990; and SLAC-PUB-5100, 1990.
- [7] M.Virchaux (BCDMS), private communication.
- [8] BCDMS: presented by M.Virchaux at the Workshop on Hadron Structure Functions and Parton Distributions, Fermilab, April 1990; and M.Virchaux, private communication.
- [9] E665: presented by C.Halliwell at this conference.
- [10] R.G.Arnold et al., Phys. Rev. Lett. 52(1984)727

DISCUSSION

J. Soffer (CPT-CNRS, Marseille): [Reference: Isospin violation in quark-parton distributions (G. Preparata, Ph. Ratcliffe, J. Soffer), post-deadline contributed paper submitted to the Conference]. The analysis of recent and accurate DIS data leads us to conclude that isospin is strongly violated in proton sea-quark distributions. Such findings have severe implications for reliable global patron distributions fitting programs.

ISOSPIN VIOLATION IN QUARK-PARTON DISTRIBUTIONS

Jacques SOFFER

Centre de Physique Théorique, CNRS-Luminy, Case 907, 13288 Marseille cedex 9, France

One of the most fundamental results of the Quark-Parton Model is the derivation of several sum-rules relating to the various deep-inelastic scattering structure functions. From their relationship to quark-parton distributions it is readily seen that these sum rules simply count the numbers of valence type quarks in certain combinations. In terms of these distributions the Adler sum-rule (ASR) [1] reads

$$\int_0^1 dx \left[u(x) - d(x) - \bar{u}(x) + \bar{d}(x) \right] = 1 \quad (1)$$

and the Gross-Llewellyn Smith sum rule (GLSSR) [2] reads

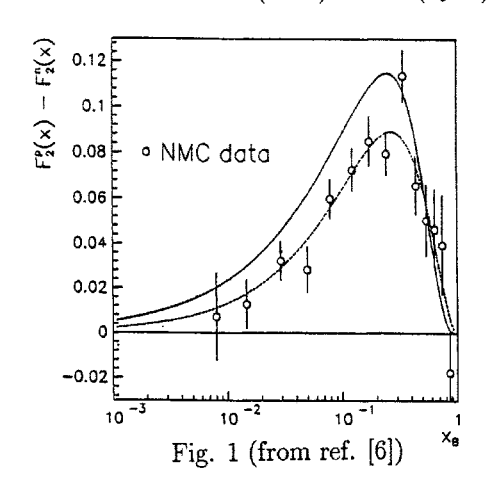
$$\int_{0}^{1} dx \left[u(x) + d(x) - \bar{u}(x) - \bar{d}(x) \right] = 3 \left(1 - \frac{\alpha_{s}}{\pi} \right)$$
 (2)

and since $q_{\text{val.}}(x) = q(x) - \bar{q}(x)$, the sea quarks don't contribute to the ASR and GLSSR. If one assumes isospin invariance in the sea, i.e. that $\bar{u}(x) = \bar{d}(x)$, a further sum-rule may be obtained from the ASR namely the Gottfried sum-rule (GSR) [3]

$$\int_0^1 \frac{dx}{x} \left[F_2^{ep}(x) - F_2^{en}(x) \right] dx = 1/3 \qquad (3)$$

Recently the NMC at CERN [4] has reported very accurate data (see fig. 1) and a preliminary value for this integral from $x_B = 0.004$ to 1 is

$$GSR = 0.230 \pm 0.013(stat.) \pm 0.027(syst.)$$
 (4)



which implies

$$\int_0^1 dx \left(\bar{d}(x) - \bar{u}(x) \right) = 0.14 \pm 0.06 \tag{5}$$

or the assumption that the GSR gets a substantial contribution from the region $x_B\langle 0.004$. The second possibility is ruled out because from the CCFR data at FNAL [5] for $xF_3(x)$ (see fig. 2) one gets

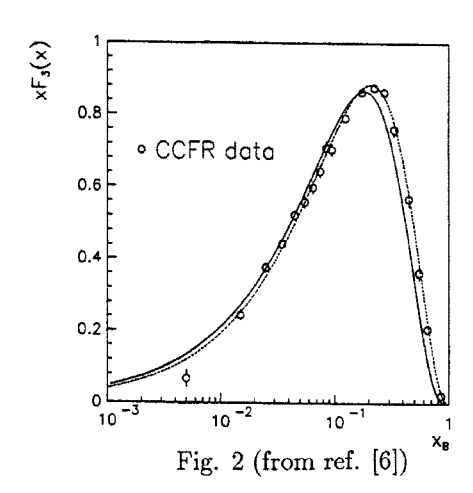
$$GLSSR = 2.66 \pm 0.03(stat.) \pm 0.08(syst.)$$
 (6)

in excellent agreement with the theoretical value (eq. (3)).

We conclude [6] that this is an evidence for a strong violation of isospin in the proton sea.

REFERENCES

- 1. S.L. Adler, Phys. Rev. 143 (1966) 1144.
- D. Gross and C. Llewellyn Smith, Nucl. Phys. B14 (1969) 337.
- 3. K. Gottfried, Phys. Rev. Lett. 18 (1967) 1154.
- 4. Jan Nassalski, New Results from F_2 structure functions, these proceedings.
- The CCFR Collab., W.C. Leung et al., presented at the XXV Rencontre de Moriond (Hadronic Interactions), March 1990.
- G. Preparata, P.G. Ratcliffe and J. Soffer, preprint Marseille CPT-90/PE.2417.



MEASUREMENT OF THE XENON/DEUTERIUM INELASTIC CROSS SECTION RATIO USING 490 GeV/c MUONS

C. HALLIWELL*

Physics Department, University of Illinois at Chicago, P.O. Box 4348, Chicago, Illinois 60680, U.S.A.

ABSTRACT

Inelastic scattering of 490 GeV μ^+ from deuterium and xenon nuclei has been studied at energy transfers (v) up to 370 GeV and four-momentum transferred squared (Q²) down to 0.1 GeV². A depletion in the inelastic μ^+ cross section has been observed from xenon compared to deuterium in the kinematic range 0.001 < x_{Bj} < 0.08. The ratio of the xenon/deuterium cross section decreases with increasing v but does not depend on Q². The data extend the v and Q² ranges studied previously in charged lepton and photoproduction experiments. The data agree qualitatively with models that invoke parton fusion in nuclei and models based on generalized vector dominance.

INTRODUCTION

Recent measurements [1,2,3] have confirmed that the yield of inelastically scattered muons per nucleon from heavy nuclei is suppressed in the low x_{Bj} region; $x_{Bj} = Q^2/2Mv$ where Q^2 and v are the four-momentum squared and energy transferred from the muon to the target and M is the target mass. This suppression, termed "shadowing", has been measured using virtual photons; it is reminiscent of earlier results obtained in photoproduction experiments [4]. New results from Fermilab experiment E665 augment these data by extending the kinematical range; this was made possible with the use of the highest energy muon beam available and a novel trigger. In addition, E665 has used the heaviest nuclei (xenon) to date [5].

APPARATUS

E665's apparatus has been described in detail elsewhere [6]. In this paper we will emphasize the elements that are relevant to the study of low Q^2 , high ν scattering, that is, the detection and measurement of muons scattered through small angles (θ).

The momentum of the incident muons was measured using a beam spectrometer consisting of multiwire proportional chambers and small scintillation hodoscopes placed upstream and downstream of a dipole magnet. The resolution of the wire chambers enabled a reconstructed momentum resolution of 0.5% at 490 GeV/c. The hodoscopes defined the incident beam for the small angle trigger (SAT) de-

scribed below. The scattered muon was identified by its presence downstream of a 3 m thick iron hadron absorber. Its momentum was measured by a forward spectrometer consisting of a large-aperture superconducting dipole magnet instrumented with proportional wire chambers and drift chambers. The momentum resolution of this spectrometer was 2.5% for a 490 GeV/c muon; this corresponds to the following range of resolutions:

	Maximum	Minimum
ν	0.8% at 375 GeV	30% at 40 GeV
Q^2	2% at 10 GeV ²	16% at 0.1 GeV ²
хвj	16% at 10 ⁻³	16% at 10 ⁻¹

Inelastic muon scattering at low Q^2 typically results in muons that remain within the geometrical phase space of the unscattered beam. An interacting muon was detected by the SAT as follows: the incident muon's trajectory was extrapolated through the forward spectrometer to a hodoscope (placed downstream of the hadron absorber) and this position was compared to the counter that had fired. The event was recorded if the difference in the two positions was at least 2 counter widths. The SAT had significant acceptance above $Q^2 = 0.1 \text{ GeV}^2$ which corresponds to a scattering angle of approximately 0.5 mr.

There was increased acceptance at high ν values and small θ . This kinematical region is dominated by events in which an incident μ loses a significant fraction of its momentum but continues travelling in its original direction. This frequently happens when

the μ undergoes bremsstrahlung in the target or when small angle $\mu\text{-e}$ scattering occurs. These two processes were the dominant backgrounds to inelastic μ scattering in the high ν , low Q^2 region. Large angle μ scattering in the hadron absorber was also a source of fake triggers. These events were rejected from the final event sample during the analysis stage by determining that no interaction had occurred in the target.

An essential role in this study was played by a large aperture electromagnetic calorimeter with fine longitudinal and transverse segmentation^[6]. This detector allowed an event-by-event detection of radiative photons which greatly reduced the uncertainty in the final corrections applied to the data sample.

DATA

Data from two targets (xenon, A=131, 8.5 gm/cm² and deuterium, 16 gm/cm²) are reported here. In addition to these, a hydrogen and an empty target vessel were used.

In Figure 1 the yield from deuterium is shown as a function of x_{B_i} with the requirement that $y = v/E_{inc} <$

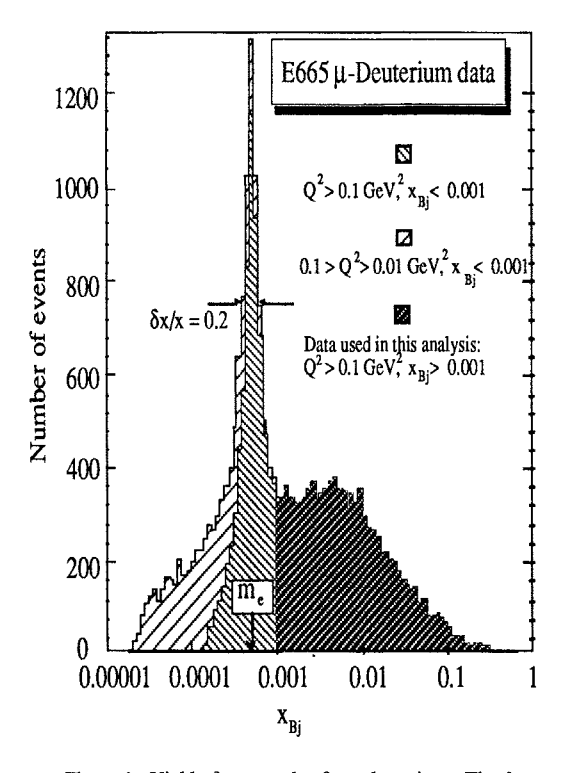


Figure 1. Yield of scattered μ from deuterium. The data in the region 10^{-4} are dominated by events with $0.01 < Q^2 < 0.1$ GeV². These data, and those corresponding to μ -e elastic scattering, were eliminated by the cut $x_{Bj} > 10^{-3}$.

0.75; this requirement eliminates the majority of bremsstrahlung events. A significant fraction of μ -e elastic scattering events survive; these events are peaked at $x_{Bj} = m_e/m_p = 1/1836$. The width of the peak is a measure of the x_{Bj} resolution (20% at $x_{Bj} = 0.0005$) and agrees with the estimated resolution obtained from chamber resolutions. The μ -e peak restricts the kinematical region which can be used to analyze deep inelastic scattering using the μ alone to $x_{Bj} > 0.001$. A final event sample comprising 10276 xenon and 9914 deuterium inelastic μ scattering events was obtained by applying the following kinematical cuts: $E_{inc} > 400$ GeV, $\nu > 40$ GeV, $\nu < 0.75$, $Q^2 > 0.1$ GeV², and $x_{Bj} > 0.001$.

CORRECTIONS

Data from deuterium and xenon were obtained in two different time periods and therefore the yields were potentially sensitive to time dependent effects in the apparatus' performance. The following is a list of the major corrections (including time dependent ones) applied to the data:

Empty target subtraction: A small fraction of events originated from material other than the xenon or deuterium targets. A correction for this was made by obtaining data from an empty target vessel with a yield of typically 4% of the full target. The correction was dependent on x_{Bj} attaining a maximum value of 15% at $x_{Bj} = 0.001$. The estimated uncertainty on the ratio of the xenon/deuterium cross section was 1%.

Normalization: Two independent methods were used to determine the beam flux. A difference of 0.7% remained after studies.

Scattered μ reconstruction: The efficiencies of the wire chambers in the forward spectrometer were time dependent which led to an uncertainty of 4% on the ratio of the cross sections.

Target density: The uncertainty in the densities of the two targets led to a potential error of 0.4% in the cross section ratio.

Radiative corrections: These corrections are especially important in the high y (low x_{Bj}) kinematical region. Up to 70% of the scattered μ yield from a μ -xenon interaction originates from radiative processes which corresponds to a 25% correction on the cross section ratio.

The corrections were performed using a two-stage process. First, the kinematical cuts mentioned in the previous section were applied; these minimized the number of bremsstrahlung and μ -e events. Second, to the remaining sample, two independent methods were 0.9 used to estimate the necessary corrections: (a) events were discarded if the electromagnetic calorimeter had detected more than 80% of the virtual photon's energy (v) and a requirement on the maximum number of energy clusters detected in the calorimeter was satisfied 0.6 (b) event yields were corrected using a calculation based on a computer program^[7].

There was consistency between the two approaches (even at high y values where the correction is large). It is estimated that a maximum systematic uncertainty of 7% remains in the radiative correction. The results presented in the following section were all produced by applying calculated radiative corrections rather than by eliminating events using data from the calorimeter. Combining all the potential uncertainties results in a maximum systematic error on the ratio of xenon/deuterium yields of ~8%.

RESULTS

The kinematics of inelastic μ scattering are described by two independent variables, the choice of which is often influenced by the physics being studied. The data in this section are presented as a function of Q^2 , ν and x_{Bj} .

The Q^2 variation of the xenon/deuterium cross section ratio per nucleon is presented in Figure 2 for an interval of x_{Bj} ; data from NA28^[1,2] for a similar x_{Bj} range are also shown. In addition, a point from photoproduction^[4] is included. E665's data increase the kinematical range previously studied and one can see that there is no evidence of a Q^2 dependence of the cross section ratio.

The v dependence of the xenon/deuterium cross section ratio is shown in Figure 3. The E665 data span a range $0.1 < Q^2 < 0.5 \text{ GeV}^2$ and are compared with NA28^[8] and photoproduction data^[4]. The E665 data are consistent with shadowing increasing with photon (real or virtual) energy; the amount of shad-

E665: σ_{Xe} / σ_{D} (0.001 < $x_{Bj} < 0.025$)

O NA28: F_{2Ca} / F_{2D} (0.004 < $x_{Bj} < 0.018$)

1

0.9

0.8

0.7

E665

preliminary data

0.1

Q² (GeV²)

Figure 2. Q^2 dependence of the E665 σ_{Xe}/σ_D cross section ratio. (solid squares) compared to NA28's^[1,2] calcium/deuterium data (open circles). The photoproduction point (shown as a shaded circle on the vertical axis) was obtained by extrapolating A_{eff}/A for Cu data^[4] to Xe. Only statistical errors are shown for the E665 data.

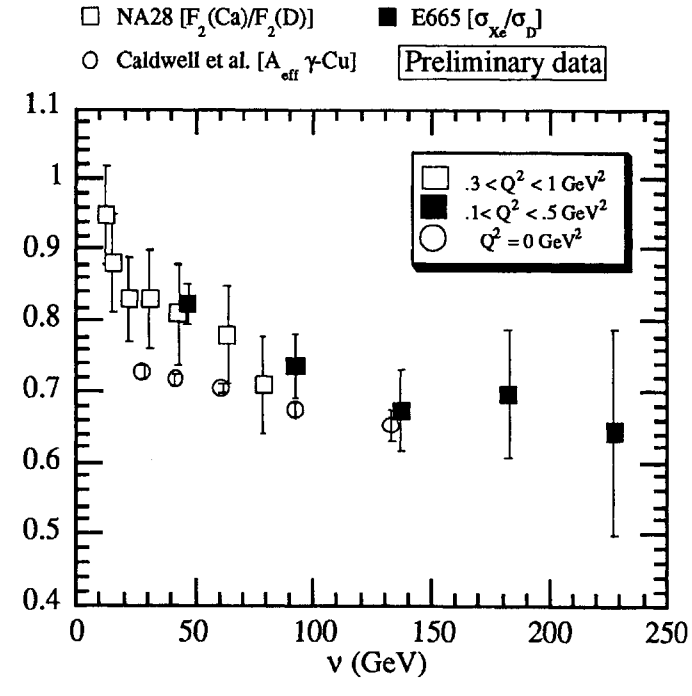


Figure 3. Energy dependence of shadowing. E665 data are shown as solid squares and are compared to NA28 data [8] (open squares) and A_{eff}/A for Cu data from photoproduction [4] (open circles). Only statistical errors are shown for the E665 data.

owing from virtual photons appears to be less than that from real photons.

The x_{Bj} variation of the data is shown in Figure 4; a strong suppression occurs as x_{Bj} decreases. E665's data are compared to structure function measurements from NA28. Increasing amounts of shadowing with

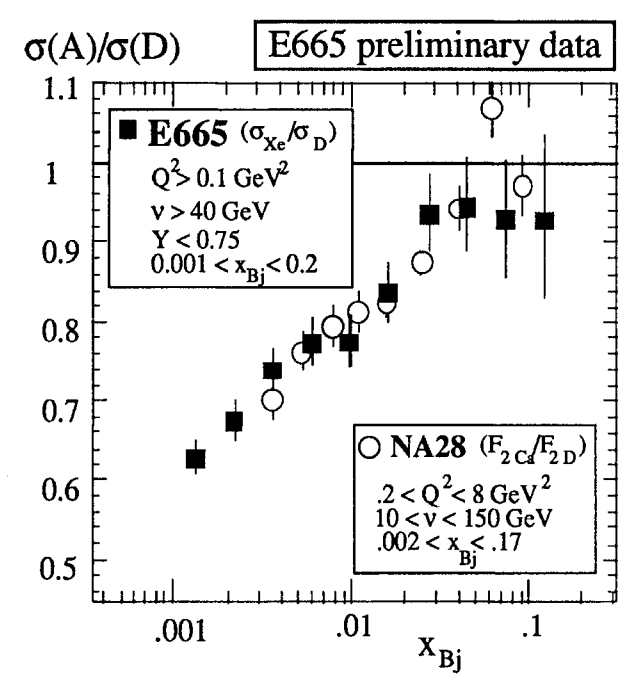


Figure 4. The $x_{\rm Bj}$ dependence of the xenon/deuterium cross section ratio. (E665 data, solid squares) and the Calcium/ deuterium structure functions (NA28 data, open circles). The estimated systematic errors are 8%. (E665) and 6% (NA28). Only statistical errors are shown for the E665 data.

atomic number, A, have been previously measured in photoproduction and μ scattering. E665's data are expected to lie somewhat below NA28's because of E665's heavier xenon target . This is not ruled out as the quoted systematic errors from the two experiments are 6% for NA28 and 8% for E665. Recent preliminary results from the high statistics NMC experiment $^{[3]}$ using calcium and deuterium targets report ratios higher than those reported by NA28. Comparing E665's data with NMC's would lead to the conclusion that shadowing continues to increase with A even for heavy nuclei such as xenon.

The E665 data in the vicinity of $x_{Bj} = 0.002$ suggest that shadowing continues to increase with decreasing x_{Bj} ; there is no evidence for "saturation".

COMPARISON WITH THEORETICAL MODELS

E665's data are consistent with an increase in shadowing with v; such a dependence is not pre-

dicted by vector meson dominance (VMD) or generalized VMD models ^[9]. Shadowing is predicted to increase until the lifetime of the vector meson fluctuation ($\tau = 2v/[Q^2 + m_V^2]$, where m_V is the mass of the vector meson) is comparable to the nuclear radius^[10]. This should occur approximately at v = 5 GeV, after which no substantial increase should take place.

There is no evidence for a Q^2 dependence of shadowing at constant x_{Bj} . This may be consistent with generalized VMD models [11,12,13]. Several parton-models based on the concept of parton recombination have been proposed[14,15,16]. Although within QCD it is expected that shadowing will decrease as Q^2 increases, this effect is expected to be offset by the increase in the density of low- x_{Bj} partons. A slow decrease in shadowing is expected as Q^2 increases[14]. E665's data supports a weaker Q^2 dependence than predicted by most parton-based models.

Many models predict shadowing for $x_{Bj} < 0.1$. However, most of them anticipate a smaller amount than is seen by the data; several also expect shadowing to saturate because of the finite thickness of nuclei. The disagreement between parton-based predictions and experimental data may be due to the theoretical calculations being performed at a fixed value of Q^2 , typically ~4 GeV². In contrast to this, the data have been averaged over a Q^2 range for each x_{Bj} value which leads to a correlation between x_{Bj} and Q^2 (for example at $x_{Bj} = 0.0013$, $<Q^2> = 0.4$ GeV² whereas at $x_{Bj} = 0.13$, $<Q^2> = 20$ GeV²).

CONCLUSIONS

New data have been presented for muons scattering inelastically from xenon and deuterium targets. The data increase the kinematical region previously studied and confirm that shadowing increases with decreasing x_{Bj} . The data support no Q^2 dependence for fixed x_{Bj} and a weak v dependence of shadowing is apparent for low Q^2 , high v photons.

ACKNOWLEDGEMENTS

The work of the University of California, San Diego was supported in part by the National Science Foundation, contract numbers PHY82-05900, PHY85-11584 and PHY88-10221; the University of Illinois at Chicago by NSF contract PHY88-11164; and the Uni-

versity of Washington by NSF contract numbers PHY83-13347 and PHY86-13003. The University of Washington was also supported by the U. S. Department of Energy. The work of Argonne National Laboratory was supported by the Department of Energy, Nuclear Physics Division, under Contract No. W-31-109-ENGGG-38. The Department of Energy, High Energy Physics Division supported the work of Harvard University, the University of Maryland, the Massachusetts Institute of Technology under Contract No. DE-AC02-76ER03069 and Yale University. The Albert-Ludwigs-Universitat and the University of Wuppertal were supported in part by the Bundesministerium fuer Forschung and Technologie.

REFERENCES

*Representing E665: M.R. Adams⁷, S. Aid⁸, P.L. Anthony⁹, M. D. Baker⁹, J.F.Bartlett⁴, A. A. Bhatti¹¹, H.M. Braun¹², W. Busza⁹, J.M. Conrad⁶, G. Coutrakon⁴, R. Davisson¹¹, I. Derado¹⁰, S.K.Dhawan ¹³, W. Dougherty ¹¹, T. Dreyer⁵, V. Eckardt¹⁰, U.Ecker¹², M. Erdmann⁵, A. Eskreys³, H.J. Gebauer¹⁰, D.F. Geesaman¹, R. Gilman¹, M.C. Green¹, J. Haas⁵, C. Halliwell⁷, J. Hanlon⁴, D. Hantke¹⁰, V.W. Hughes¹³, G. Jansco¹⁰, H.E. Jackson¹, D.E. Jaffe⁷, D.M. Jansen^{ll}, S. Kaufman^l, R.D. Kennedy², T. Kirk⁴, H.G.E. Kobra k², S.Krzywdzinski^{ll}, S. Kunoni⁸, J.J. Lord^{ll},H.J. Lubatti^{ll}, T. Lyons⁹, S.Magill⁷, P. Malecki³, A. Manz¹⁰, D. McLeod⁷, H. Melanson⁴, D.G. Michael⁶, W. Mohr⁵, H. E. Montgomery⁴, J. G. Morfin⁴, R. B. Nickerson⁶, S. O'Day⁸, L. Osborne⁹, B. Pawlik³, F.M. Pipkin⁶, E.J. Ramberg⁸, A. Roser¹², J. Ryan⁹, A. Salvarani², M. Schmitt⁶, N. Schmitz¹⁰, K. P.Schuler¹³, H.J. Seyerlein¹⁰, A. Skuja⁸, G. Snow⁸, S. Soldner-Rembold¹⁰, P.H. Steinberg⁸, H.E. Stier⁵, P. Stopa³, R. A. Swanson², S. Tentindo-Repond¹, H.-J. Trost¹, H. Venkataramania ¹³, M. Wilhelm⁵, J. Wilkes¹, R. Wilson⁶, W. Wittek¹⁰, S. Wolbers⁴, T. Zhao11

¹ Argonne National Laboratory, IL USA, ² University of California, San Diego, CA USA, ³ Institute of Nuclear Physics, Cracow, Poland, ⁴ Fermi National Accelerator Laboratory, IL USA, ⁵ Albert Ludwigs Universitat, Freiburg i. Br., W. Germany, ⁶ Harvard University, MA USA, ⁷ University of Illinois at Chicago, IL USA, ⁸ University of Maryland, College Park, MD USA, ⁹ Massachusetts Institute of Technology, MA USA, ¹⁰ Max Planck Institute for Physics & Astro-

physics, Munich, W. Germany, ¹¹ University of Washington, Seattle, WA USA, ¹² University of Wuppertal, W. Germany, ¹³ Yale University, CT USA

- [1] A. Ameodo et al., Nucl. Phys. B333 (1990) 1
- [2] A. Ameodo et al., Phys. Lett. B211 (1988) 493
- [3]"New Results from F₂ Structure Functions" presented by J. Nassalski at this conference.
- [4] D. O. Caldwell et al, *Phys. Rev. Lett.* **42** (1979) 553. For the comparisons made here the 60 GeV C, Cu and Pb data were interpolated to obtain a Xe value. This value was extrapolated from 60 to 150 GeV using the energy dependence of the Cu data.
- [5] μ -Pb interactions have been studied previously in a low-statistics experiment, see M. Goodman et al., *Phys. Rev. Lett.*, 47 (1981) 293
- [6] M. R. Adams et al., Nucl. Inst and Meth., A291 (1990) 533
- [7] The GAMRAD computer program is based on the calculations by L.W. Mo and Y.S. Tsai, *Rev. Mod. Phys.*, **41** (1969)
- [8] The x_{Bj} and Q^2 dependences of the data from Refs. 1 and 2 were converted into variation with v by using $\langle v \rangle = \langle Q^2 \rangle / 2Mx_{Bj}$.
- [9] G. Grammer and J.D Sullivan, in *Electromagnetic* interactions of hadrons, ed. A. Donnachie and J.Shaw (Plenum Press, New York, 1978)
- [10] T.H. Bauer, R.D. Spital, D.R. Yennie and F.M. Pipkin, "The Hadronic Properties of the Photon in High-energy Interactions", *Rev. Mod. Phys.*, **50** (1978) 261
- [11] D. Schildnecht, Nucl. Phys. B66 (1973) 398
- [12] C. L. Bilchak et al., Phys. Lett., B214 (1988) 441
- [13] C. L. Bilchak et al., Phys. Lett., B233 (1989) 461
- [14] J. Qiu, Nucl. Phys. **B291** (1987) 746
- [15] A. H. Mueller and J. Qiu, Nucl. Phys. B268 (1988) 427
- [16] F. E. Close et al., Phys. Rev., **D50** (1989)
- [17] S. J. Brodsky and H.J. Lu, *Phys. Rev. Lett.*, **64** (1990)

PARTON DISTRIBUTIONS FROM A GLOBAL QCD ANALYSIS *†

Wu-Ki Tunga,b and Jorge G. Morfinb

^a Department of Physics, Illinois Institute of Technology, Chicago, Illinois 60616, U.S.A. ^b Fermi National Accelerator Laboratory, P.O. Box 500, Batavia, Illinois 60510

ABSTRACT

Parton Distribution Functions consistent with neutrino and muon deep inelastic scattering and Drell-Yan pair production data have been extracted. This analysis incorporates experimental systematic errors and heavy target corrections; and explores the dependence of the results on kinematic cuts in the data, and choice of initial functional form. Extracted parton distribution sets are parametrized in a compact form, and are presented both in the DIS and MS-bar renormalization schemes. The form adopted is motivated by perturbative QCD and suitable for exploring the small-x behavior of the distributions. This is crucial for studying the range of predictions for Collider, HERA, and SSC/LHC cross sections.

Introduction

The QCD Parton Model provides a comprehensive framework for describing general high energy processes in current and planned accelerators and colliders. In this framework, the cross-section $\sigma_{AB\to C}$ for a hadron-hadron collision process $A+B\to C+X$, where C represents a final state of physical interest, is written as the convolution of a set of universal Parton Distribution Functions $f_A^a(x,Q)$ and parton-initiated fundamental hard cross-sections $\sigma_{ab\to C}$.

The process-independent parton distributions are the key link between the physically measured crosssections $\sigma_{AB\to C}$ and the basic processes of the theory $\sigma_{ab\to C}$. The precise determination of these functions are of fundamental importance for the interpretation of experimental results within the Standard Model and in any search for "new physics". [1] Renewed current interest in this subject is motivated by: (i) "precision studies" of the SM where the largest sources of uncertainty are often associated with the input parton distributions, especially the sea-quarks; (ii) the study of dominant QCD jet production and heavy flavor production processes (both in their own right and as background in search of new physics) for which good knowledge of the gluon distribution is still lacking; and (iii) active studies of HERA, LHC and SSC physics for which a good handle on the small-x behavior of the parton distributions is a key ingredient which is missing.

Several well-known parametrizations [2] of parton distributions extracted from early experimental data and using leading order QCD formalism have long been in wide use. Analyses based on more current data and incorporating next-to-leading order QCD evolution of the distribution functions have also recently become available^[3]. However, most of these analyses use only limited sets of data, some of which have since been significantly revised. Most of these analyses do not include experimental systematic errors or explore the dependence of the results on such factors as kinematic cuts in the analysed data, heavy target corrections, choice of initial functional forms, etc. Since most modern applications of the QCD Parton Model either require a high degree of accuracy or involve extrapolation of the kinematic variables (x, Q) well beyond the measured range, all these factors can significantly affect the predictions.

A comprehensive review of the current status of DIS experiments and parton distribution analyses including a plan to compile an extensive database and to investigate all the relevant factors in such analyses was given at the 1988 Snowmass Workshop [4] We report here first results of this global analyis and present representative parton distribution sets with a range of different behaviors in a simple and easy-to-use form. Finally, we discuss some of the physical consequences in current collider processes, as well as projections for HERA and SSC energies. Details of this work can be found in a forthcoming publication [5].

^{*}Presented by Wu-Ki Tung

[†]Supported in part by NSF Grant No. PHY89-05161

Functional Form of Distributions

Although there is no real theory on the correct functional form of the parton distributions in the framework of QCD, the natural occurrance of logarithmic factors in perturbative quantum field theory lead us to adopt the ansatz:

$$f(x,Q) = e^{A_0} x^{A_1} (1-x)^{A_2} \log^{A_3} (1+\frac{1}{x}) \qquad (0.1)$$

Here, for clarity, we have suppressed a parton flavor label. The A-coefficients will be referred to as "shape parameters" in our data-analysis. The important advantages of this parametrization are: (i) it is suited to represent f(x,Q) for all Q, thus reduce the special role of the arbitrarily chosen Q_0 for the initial distribution; (ii) it is guaranteed to be positive definite and it is smooth in both variables, and iii) it provides a simple and versatile way to study the small-x behavior of the parton distributions. By selectively choosing A_1 and/or A_3 as active parameters, we can use existing data to explore the full range of power- and/or logarithmic-law small-x extrapolations of the parton distributions from the current range. (Cf. the section on small-x extrapolation of parton distributions later.)

Data Analysis

The D.I.S. data sets included in this analysis are CDHSW^[6] neutrino scattering results in conjunction with EMC^[7] and BCDMS^[8] muon scattering experiments. These data sets were used in various combinations to test both the consistency of the experimental results and the stability of the fitting results. All calculations reported below use the full 2-loop evolved parton distributions and the appropriate 1-loop Wilson coefficients for the structure functions.

We examined the stability of fitting results as the values of Q^2 - and W- cuts are varied; and determined that, without a priori knowledge of higher twist contributions, consistent results are obtained with $Q^2 > 10 GeV^2$ and W > 4 GeV. These default cutoff values preserve the bulk of the high statistics data and decrease any possible contamination of higher twist effects by at least a factor of 4 compared to most recent global analyses. It is, of course, imperative to include the experimental systematic errors, especially when data from several different high statistics experiments are included. We also make corrections for the "EMC" effect for scattering data on heavy targets.

We next include lepton-pair production (Drell-Yan process) data from the Fermilab E288^[10] and E605^[11] experiments. These data are particularly

sensitive to the product of the u and \overline{u} distributions. They provide a useful handle on the sea-quark (\overline{u}) . In addition, the gluon distribution comes in here in a direct way—as we are performing a next-to-leading order analysis.

With the combined D.I.S. and D-Y data used in our analysis, we consistently get good overall fits with 10 - 11 independent shape parameters. In addition to the inclusion of point-to-point systematic errors. our fits incorperate an overall relative normalization factor for each experimental data set. The relative normalization factors obtained in these combined fits (+8% for EMC and -2% for BCDMS) agree quite well with those found independently by recent critical comparisons and reviews of these experiments^[12]. With our usual choice of Q2-cut (10GeV2), W-cut (4GeV), and error handling (systematic and statistical added in quadrature), the global fits to the BCDMS H2 & D2, CDHSW, and the E288 & E605, data (referred to henceforth as the "B-fits") involve 647 data points. The overall χ^2/dof for these fits is on the order of 0.8 and evenly distributed among the data sets - indicating a large degree of consistency among these different physical measurements in the QCD framework. Correspondingly, the global fits to the EMC H2 & D2, CDHSW, and the E288 & E605 data with the same choice of kinematic cuts and error handling, (referred to henceforth as the E-fits) involve 472 data points; the overall χ^2 per degree of freedom is typically around 0.93. The χ^2 of the individual data sets varies between 0.65 - 0.85 for all sets except for the EMC D2 data set where it is around 1.5. Finally, the global fits to ALL the data combined (referred to as the S-fits) involve 828 data points. The overall χ^2/dof range is 0.94 -0.97; the χ^2/dof for the individual data sets are not as consistently distributed as for the B and E fits with the χ^2/dof for the EMC data sets about a factor of two higher than the rest. To illustrate the quality of these fits, we show one of them (the S-fit) compared to a subset of CDHSW data on $F_2(x,Q)$ and the D-Y data set (E605) in Fig. 1. (Cf.Fig. 2 for comparison with the BCDMS data.)

It should be mentioned that the data used in this analysis is not sufficient to differentiate the various sea-quark flavors or to independently probe the gluon. Thus, certain assumptions on the sea-quarks (e.g. SU(2) or SU(3) flavor symmetry) and gluon and sea-quark shape parameters must be made. Improved quality data from direct photon production [13] and W- and Z- production as well as semi-inclusive deep inelastic scattering, such as charm-production,

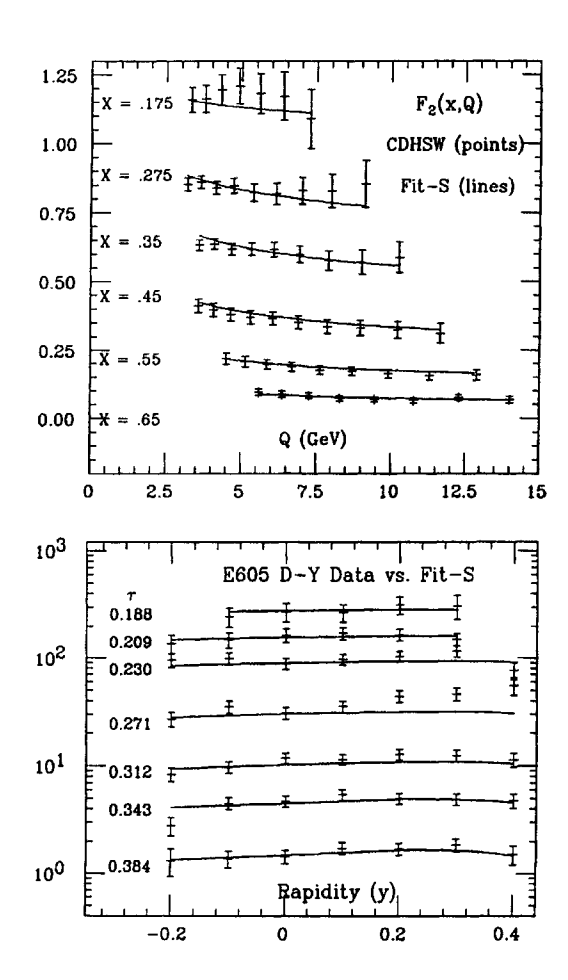


Figure 1: Fit-S compared to CDHSW $F_2(x,Q)$ and E605 D-Y data

will eventually furnish independent information on the gluon and individual sea-quark distributions, hence allow the unconstrained determination of these distributions

Comparisons with Existing Distributions

To compare our global fits to D.I.S. and D-Y data with previously published sets of parton distribution functions, we have to bear in mind that some crucial data sets used in earlier analyses have been significantly revised (e.g. compare the 1983 CDHS data^[14] with the new CDHSW results.^[6]); and that the very high statistics BCDMS muon data are not used by most existing published parton distribution sets. Thus, such distributions should not be expected to fit current accurate D.I.S. data to within the experimental errors. Fig. 2 illustrate this fact by compar-

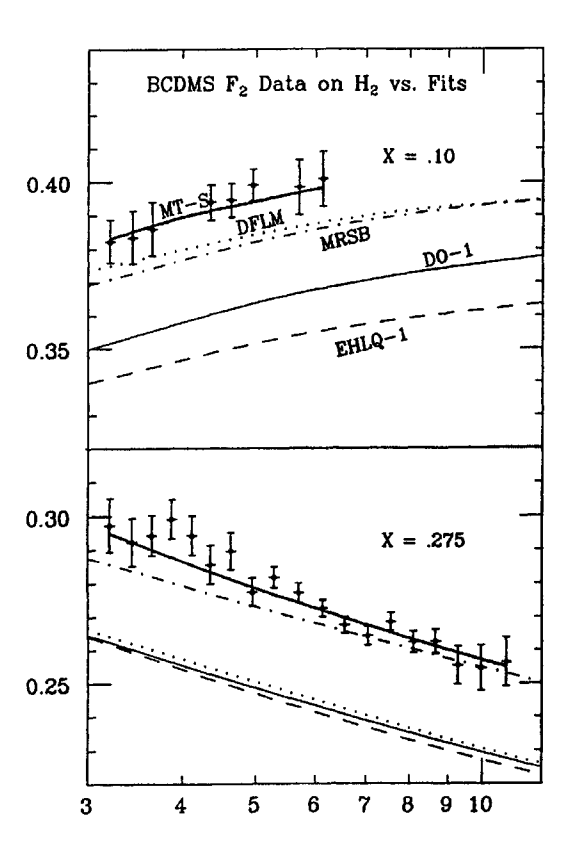


Figure 2: Comparison of subset of BCDMS data with published parton sets.

ing a representative group of BCDMS hydrogen data with the structure function F_2 calculated from the following parton distributions: our B1 set (dark-solid), EHLQ-1 (dashed), Duke-Owens-1 (light-solid), MRSB (dashdotted), and DFLM-NLLA (dotted). Note that, of the last four sets, only MRSB used (an earlier version of) the BCDMS data in their analysis. This plot illustrates that for QCD parton model studies requiring accuracy, the earlier well-known parton distribution sets are no longer sufficient. The fact that the DFLM set was obtained without using the muon data also clearly shows in this plot.

Any direct comparison of distinct sets of parton distributions themselves must take into account the precise definition of the distribution function adopted as, in next-to-leading order of QCD, these quantities depend critically on the renormalization scheme used. The shape of the gluon distribution, in particular, depend sensitively on the choice of scheme, as the conversion formula contains a term from radiating valence quarks which can be quite important at large

x. (cf. Ref^[5]) Of the two recent published analyses, the DFLM sets are in the so-called DIS scheme (in which the gluon contribution to the total inclusive F_2 structure function is, by definition, absorbed into the quark distributions), whereas the MRS sets are in the ("universal") MS-bar scheme. In our analysis, we use the DIS scheme distributions in the fitting process for the practical reason that the comparison with F_2 data, which dominate the fit, is made very simple. The results of these analyses, however, can be presented in any scheme with the proper transformation applied.

Parametrization of Results

One of the important motivations for adopting the functional form, Eq.(0.1) is that it is naturally suited to represent the parton distributions at any value of Q. Thus, although involved numerical methods are used in generating the parton distributions, it is possible to re-express all the final results in this simple functional form for any given Q. The QCD-evolution of the distribution functions then manifests itself in Q-dependent A-coefficients. Because the natual evolution variable is $\log(\log(Q))$, we can expect rather weak Q-dependence of these coefficients which are then easily parametrized by simple functions. Hence we represent our parton distributions in the form (0.1), and parametrize the A-coefficients for each parton flavor as:

$$A^{i}(Q) = C_{0}^{i} + C_{1}^{i}T(Q) + C_{2}^{i}T(Q)^{2}; \qquad (0.2)$$

where $T(Q) = \log(\log \frac{Q}{\Lambda}/\log \frac{Q_0}{\Lambda})$ and i = 0 - 3. The constant coefficients are determined by an overall fit to the particular parton distribution function over the range $(10^{-5} < x < 1, 3 GeV < Q < 10^4 GeV)$. The resulting parametrization proves to be accurate to within the same degree as the original fit to data, thus it is a faithful representation of fitting results. This means each set of parton distributions is specified by a compact table of the C-coefficients. Tables of such coefficients for the fits mentioned above can be found in Ref. [5]

Small-x Extrapolation

We explore the small-x behavior of the parton distributions, which are consistent with current data, in two different ways which distinguish our approach from previous efforts. First, we leave the parameter A_1 (cf. Eq.(0.1)) for the gluon and sea-quarks as a free parameter in the data analysis, hence its value (at a fixed value Q_0) is determined by the data rather than by an

arbitrary assumption. Since the effective power A_1 changes rapidly with Q in the relatively low Q region where evolution starts, any assumption one makes is highly dependent on the choice of Q_0 . Our method does not prejudice this choice. Secondly, by introducing a logarithmic factor $(\log x)^{A_3}$ in the functional form, Eq.(0.1), we allow for the possibility of logarithmic extrapolation to the small-x region in addition to the traditional power-law extrapolation. This is logical, as the evolution equation naturally introduces logarithmic dependences of the parton distributions even if one starts with a pure power-law function.

For a given selection of data sets we routinely perform fits with the A_1 factor alone, with the A_3 factor alone, and with both as fitting parameters. Since available data in D.I.S. and D-Y processes involve a limited range in x, we are able to get good fits in all three cases. Within the (x,Q) range of current experiments the resulting parton distribution sets yield very similar D.I.S. structure functions and D-Y cross-sections; but they lead to different predictions far away from this range, especially for very small x. In this way, we can study the range of small-x behavior of parton distributions allowed by current data in a systematic and quantitative way.

For illustration, in Fig. 3a we plot the structure function F_2 and the gluon distribution at $Q^2 = 10 GeV^2$ in the x-range $(10^{-5}, 10^{-1})$. The two representative parton distribution sets "B1" and "B2" both fit the existing data (x > 0.03) but they have different $A_1 - A_3$ exponents which give rise to quite different predictions in the x < 0.03 range. In Fig. 3b the same quantities are plotted at $Q^2 = 10^4 GeV$. As expected, there is a migration of the partons to small x caused by the Q^2 evolution, so that differences are reduced as Q^2 increases.

Since the HERA experiments are expected to measure the structure functions down to $x=10^{-4}$, Fig. 3 illustrates how these experiments can contribute to narrow the uncertainties as they exist now. Before these distributions are measured at HERA, "predictions" on cross-sections for various processes at SSC and LHC which depend on parton distributions at small x have to be considered in the context of the uncertainties described here.

In Fig. 4 we show next-to-leading order calculation of the y-distribution of lepton-pairs (D-Y) at the Tevatron energy for dimuon mass Q=20 GeV using the B1, B2 parton distributions along with MRSB and DFLM-NLLA. Here we see a dramatic difference, especially between the prediction of the B2-fit distributions

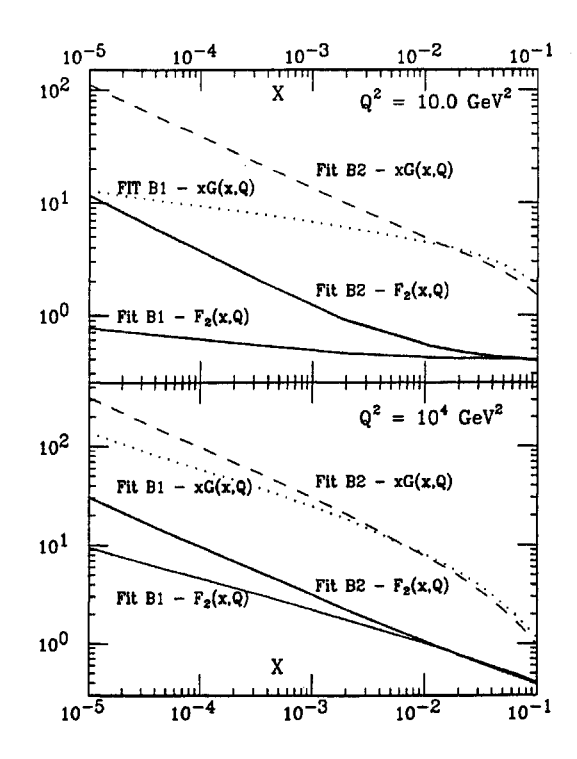


Figure 3: Small-x extrapolation of xG(x,Q) and $F_2(x,Q)$

and the rest at high y values. This sensitivity is due to the contribution of the small-x parton distributions to the D-Y cross-section — especially in the forward-backward directions. This striking effect has been known for some time, based on crude inputs [15]. The current calculation, using parton distributions known to be consistent with all current experiments, underlines the importance of the collider lepton-pair measurements in probing parton distributions at small-x.

REFERENCES

- Proceedings of Workshop on Hadron Structure Functions and Parton Distributions, Fermilab, April 1990, Ed. D. Geesaman et al, World Scientific Pub. (1990).
- M. Glueck et al., Z. Phys. C13 119 (1982); D. Duke and J. Owens, Phys. Rev. D30 49 (1984);
 E. Eichten et al., Rev. Mod. Phys. 56 579 (1984) and Erratum 58 1065 (1986).
- M. Diemoz et al., Z. Phys. C39 21 (1988); A.D. Martin, R.G. Roberts & W.J. Stirling, Phys. Rev. D37 1161 (1988), Mod. Phys. Lett. A4 1135

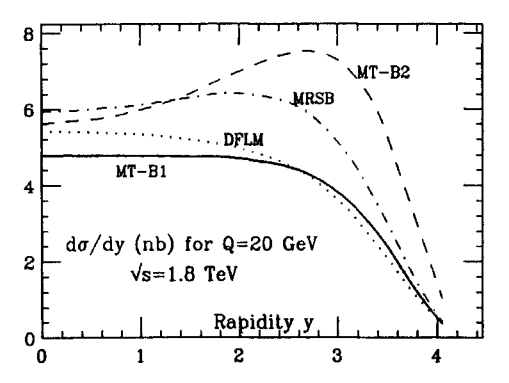


Figure 4: Prediction of y-distribution of DY crosssection

(1989).

- 4. W-K. Tung et al., "Structure Functions and Parton Distributions". in Proceedings of the 1988 Summer Study on High Energy Physics in the 1990's, World Scientific, 1989.
- 5. Jorge Morfin and Wu-Ki Tung, Fermilab-Pub-90/74 (to appear in Z. Phys. C).
- 6. J.P.Berge et al., Preprint CERN-EP/89-103 (1989).
- 7. J.J.Aubert et al., Nucl. Phys. B293 740 (1987).
- 8. A.C. Benvenuti et al., Phys. Lett. **B223** 485 (1989) and CERN-EP/89-170,171, 1989.
- K. Lang et al, Z. Phys. C33, 483 (1987); S.R. Mishra et al, in Proceedings of 14th Rencontres de Moriond, Mar. 1889.
- 10. A.S.Ito et al., Phys. Rev. D23 604 (1981).
- 11. C.N. Brown et al., Phys. ReV. Lett. 63 371 (1988).
- 12. A. Milsztajn, in Ref. 1; See also J. Feltesse, in the Proceedings of the XIV International Symposium on Lepton and Photon Interactions, Stanford, August 1989, Pub. World Scientific.
- Aurenche et al, Phys. Rev. D39, 3275 (1989). See also P.N. Harriman et al., Phys. Rev. D42, 798 (1990).
- Abramowicz et al, Z. Phys. C17, 283 (1984); Z. Phys. C25, 29 (1984); Z. Phys. C35, 443 (1984)
- F. Olness and Wu-Ki Tung, "Small x Physics at the SSC and the Tevatron" in From Colliders to Super Colliders, ed. V. Varger and F. Halzen, World Scientific (1987)

A QCD analysis of high statistics F_2 data on H_2 and D_2 targets, with determination of higher twists

A. Ouraou

D.Ph.P.E., C.E.N. Saclay, 91191 Gif-sur-Yvette Cedex (France)

Abstract We present the preliminary results of a QCD analysis of the high statistics BCDMS and SLAC F_2 data on H_2 and D_2 . At high Q^2 , the data are in good agreement with the predictions of perturbative QCD and lead to an improved measurement of Λ_{QCD} and α_S . At lower Q^2 , a precise measurement of non-perturbative effects ("higher-twists") is obtained: they are very small below x=0.40 and small, positive and increasing with x at higher x. Altogether, the data give a clear indication for the running of α_S .

In the past months, the final results of the two highest statistics measurements of F₂ on deuterium and hydrogen targets have been presented. This set of results covers a wide kinematic range: 0.07 to 0.85 in x and 0.5 to 260 GeV² in Q². These data are thus well suited for a test of perturbative QCD as well as for a measurement of possible "higher-twist" (non-perturbative) effects in the Q²-evolution of F₂. We present here the preliminary results of such a study.

The high Q² data (7 to 260 GeV²) are those obtained by the BCDMS Collaboration [1] with their muon scattering experiment using a toroidal iron spectrometer; these data have already been used for QCD analyses of F_2 [2] at high Q^2 , where nonperturbative effects are expected to be small. The low Q² data (0.5 to 30 GeV²) come from a coherent global reanalysis of electron scattering data from a number of experiments at SLAC spanning the time period 1970 to 1985 [3]. The main improvements compared to previous publications are a better determination of R(x, Q²) and a correct treatment of radiative corrections. This allows to increase the useable kinematical range. In the present analysis, we have used all the published data, apart from the last x-bin (0.85), where only SLAC data exist.

The data are shown in Figure 1, interpolated where necessary to the x-bins used here. The errors shown on Figure 1 are "total" errors, i.e. statistical and systematic combined in quadrature. In addition to these point-to-point errors, there are global normalisation errors of 3% and 2% respectively for the BCDMS and SLAC data. We do not discuss here the comparison and compatibility of these data sets, which

can be found in [4]. We nevertheless emphasize a specific point from ref. [4] that is important for the treatment of systematic errors in our fits: the kinematical region where the systematic errors are largest in the muon scattering data corresponds to high x (x > 0.50) and low Q^2 . In this region, the systematic error originates predominantly from uncertainties on the calibrations of the measurement of the incident and scattered muon energy and on the resolution of the spectrometer. These three sources of errors have a similar x and Q2 dependence and can thus be combined quadratically into a one-standarddeviation 100% correlated error which we call here the "main systematic error" of the BCDMS data (see [5] for full tables of errors and [4] for a more detailed discussion). Unfortunately, this dominant systematic error is largest precisely where the low Q2 SLAC and high Q² BCDMS data overlap to some extent.

We have employed for these fits a computer program developed by members of the BCDMS Collaboration [6] that has already been used to fit the predictions of perturbative QCD to the BCDMS data (see e.g. [2]). This program performs a fully numerical integration of the Altarelli-Parisi equations (both singlet and non-singlet in next-to-leading order).

The free parameters in these fits correspond to

- a description of the x-dependence of the non-singlet and singlet part of $F_2(F_2^{NS}(x,Q_0^2))$ and $F_2^{SI}(x,Q_0^2))$, and of the gluon distribution $xG(x,Q_0^2)$, where Q_0^2 is taken to be 20 GeV² and

$$xG(x,Q_0^2) = 0.48(1+\eta)(1-x)^{\eta}$$

with η fixed to 7 (when free, the typical error on this exponent is ± 2 , and the fits are not sensitive to the gluon distribution above x = 0.30).

- the value of $\Lambda_{\overline{MS}}^{(4)}$ for four active quark flavours,
- coefficients C_i (one per x-bin and by target material) describing the twist-four effects (HT) in the Q^2 -evolution of F_2 , such that

$$F_2^{HT}(x_i, Q^2) = F_2^{LT}(x_i, Q^2)(1 + C_i/Q^2),$$

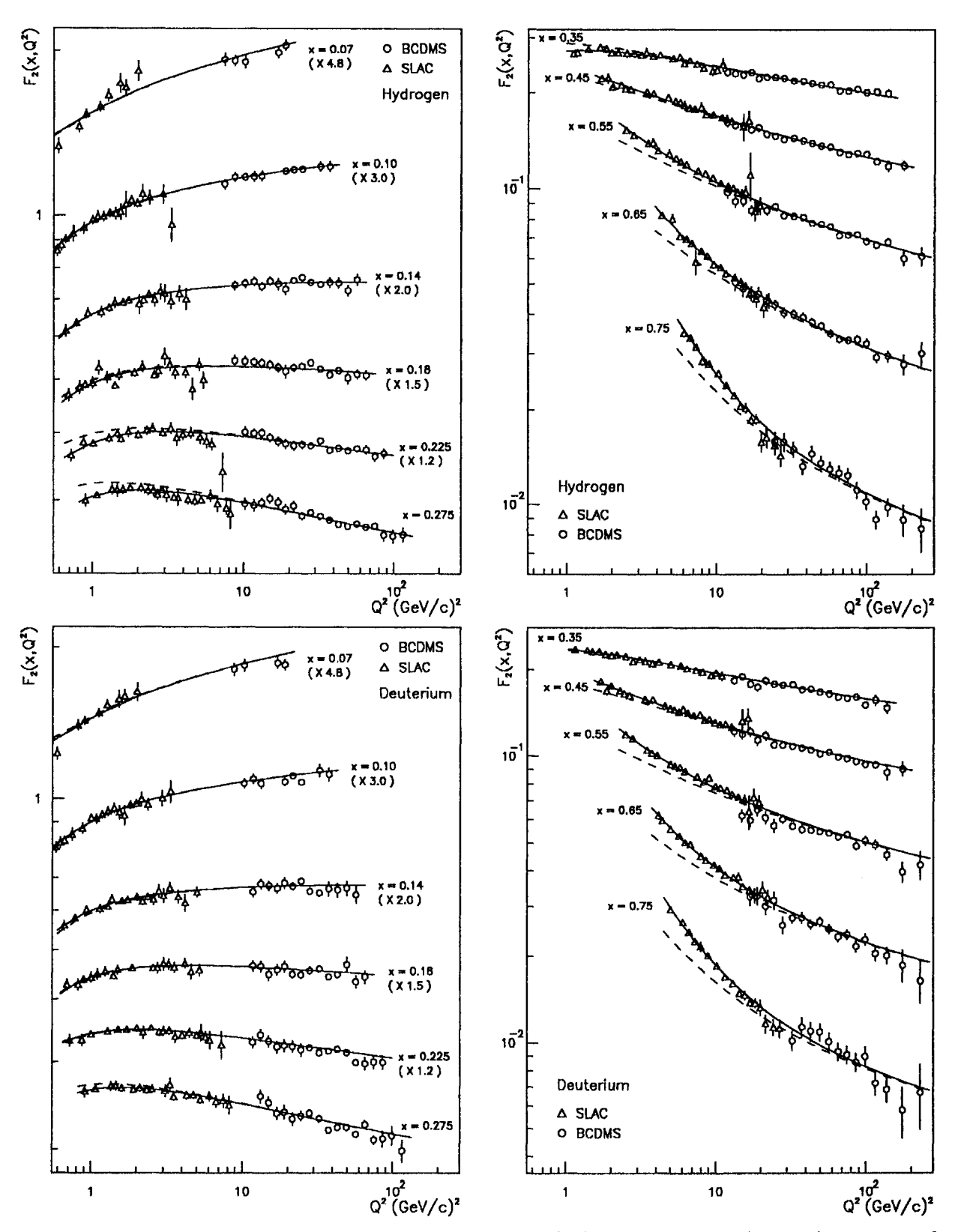


Figure 1: High statistics measurements of F₂ on hydrogen (up) and deuterium (bottom) targets. The fits shown are described in the text.

where F_2^{HT} is the function that is fitted to the data and F_2^{LT} obeys the perturbative QCD Q^2 -evolution according to Altarelli-Parisi equations.

In addition to these phenomenological and theoretical parameters that enter in the fit, we include four (two for each target material) "experimental" parameters describing the systematic errors

- one for the relative normalisation of the SLAC and BCDMS data sets,
- one for the dominant systematic error of the BCDMS data discussed above. In that case, we have taken into account all correlation effects; more explicitly, if $F_2(x_i, Q_j^2)$ and $\Delta F_2^{*y*}(x_i, Q_j^2)$ are respectively the values of F_2 and of the (one standard deviation) dominant systematic error in each bin (x_i, Q_j^2) , then the fitted quantity is $F_2(x_i, Q_j^2) + \lambda \Delta F_2^{*y*}(x_i, Q_j^2)$, where λ is the free parameter describing the "amount of BCDMS dominant systematic error".

All the other sources of systematic error in the BCDMS and SLAC data are notably smaller (comparable to or smaller than the statistical error) and we have chosen to combine them quadratically with the statistical errors, and to use the resulting errors in the fits as if they were purely statistical. We thus ignore their possible correlations but this is of minor importance given their sizes.

The QCD fits described above have been performed simultaneously on the H₂ and D₂ data and both with and without the inclusion of target mass corrections (TMC, from reference [7]). These corrections are computed numerically from the measured F₂'s themselves and do not involve any additional free parameter. The results of the fits with TMC are summarized in Table 1.

	Hydrogen	Deuterium
Λ	250 ± 40 MeV	
χ^2 / dof	(325+270)	/ (378+360-49)
BCDMS/SLAC rel. norm.	-1.0%	0.2%
λ (BCDMS main syst.)	1.5	1.3

Table 1: Results of combined QCD (NLO) fits to BCDMS and SLAC data

We now comment on the general features of these (preliminary) fit results. The χ^2 's are good - smaller than one per degree of freedom, partly because we

have included some of the systematic errors in the total errors. They are slightly better with TMC included, but this is not very significant. As an example of the fit quality, we show in Figure 1 the fit including TMC. The solid lines represent the full fit, while the dashed lines represent the leading twist contribution (F_2^{LT}). The overall description of the data by the fit is good. It is clear, from the difference between the solid and dashed curves that the influence of twistfour terms in the Q^2 -evolution of F_2 are negligible above $\sim 2~{\rm GeV}^2$ at low x (x < 0.30) and $\sim 10~{\rm GeV}^2$ at higher x.

The value of $\Lambda_{\overline{MS}}^{(4)}$ is almost the same in the two fits (it is here rounded to the nearest 10 MeV), and the total error on Λ is rather small (40 MeV): in terms of α_S , we get:

$$\alpha_S(50 \text{ GeV}^2) = 0.177 \pm 0.008.$$

This corresponds to:

$$\alpha_S(M_Z^2) = 0.112 \pm 0.003$$
 (total error).

The recent results from the LEP experiments (typically 0.118 ± 0.012 [8]) are in agreement with this value. Our error on Λ is dominated by systematic errors. The central value of 250 MeV is in agreement with recent measurements of Λ at high Q² [2]. The relative normalisation of the two data sets is everywhere smaller than 1.0% perfectly compatible with the absolute normalisation uncertainties of 3% and 2% on the BCDMS and SLAC data. The amount of BCDMS main systematic error (λ parameter) that corresponds to the best χ^2 is of order 1.4 times the published errors.

We illustrate the good agreement between the measured Q^2 -evolution of F_2 and the one predicted by perturbative QCD on Figure 2. In this Figure, the points represent the values of the logarithmic derivatives $dlnF_2/dlnQ^2$ for the hydrogen data at high Q^2 (larger than 8 to 20 GeV², depending on x), and the solid line is the prediction obtained from the fit (with $\Lambda_{\overline{MS}}^{(4)} = 250 \ MeV$). The dashed line corresponds to the fit result where the higher-twist coefficients C_i are arbitrarily put to zero: this fit is also in good agreement with the data (at high Q^2). The dotted line corresponds to the fit with no higher-twists and no target mass corrections: the difference is visible for x > 0.55. Our conclusions on the Deuterium data are similar.

In Figure 3, we show the values of the coefficients C_i , both for H_2 and D_2 , with and without inclusion

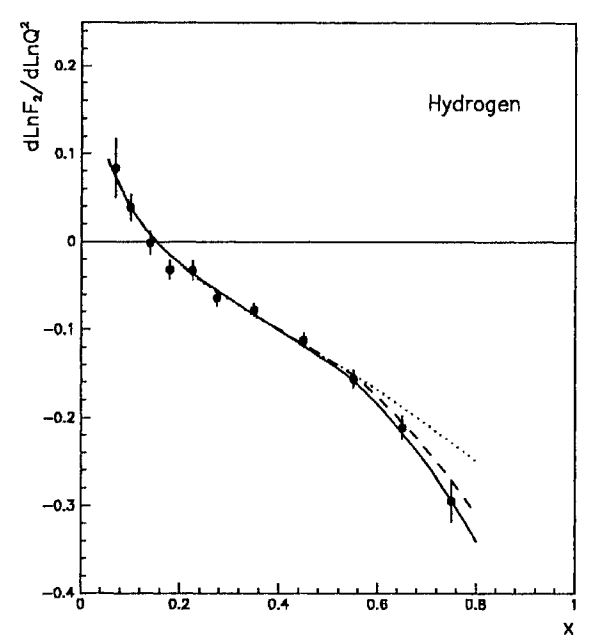


Figure 2: The logarithmic derivatives $dlnF_2/dlnQ^2$ at high Q^2 for the H_2 data. The solid line is the QCD prediction from the fit with HT and TMC (dashed line: TMC and no HT; dotted line: no TMC and no HT) for $\Lambda=250$ MeV.

of TMC's. The x-dependences of these higher-twist terms are very similar in H_2 and D_2 data. They are small for x < 0.40, and even almost compatible with zero for fits with TMC's. As the C_i parameters are nearly mutually uncorrelated in the fits, this fact is of clear physical significance. For x > 0.40, the higher-twist terms increase with x, as expected; they are clearly smaller in the case of fits including TMC's. Because of the high statistical power of these data, this determination of higher-twist terms in deep inelastic scattering is presently the most precise. We consider remarkable the fact that the inclusion of TMC's in the fits reduces everywhere the magnitude of the higher-twist terms needed to describe the data, especially so at low x where this reduction is almost a cancellation.

The behaviour of these higher-twist terms has two interesting consequences: first, concerning the large x domain (x > 0.25), the values of $\Lambda_{\overline{MS}}$ resulting from QCD fits on high Q² data (Q² > 20 GeV²) are not significantly affected by these higher-twist terms; second, concerning the lower x domain, the higher-twist influence on the Q²-evolution of F₂ is so small that even data at rather low Q² (down to 1 GeV²) can be used in the estimation of the gluon distribution.

Finally, we have performed pseudo-QCD fits to the same data, identical to the previous ones apart from

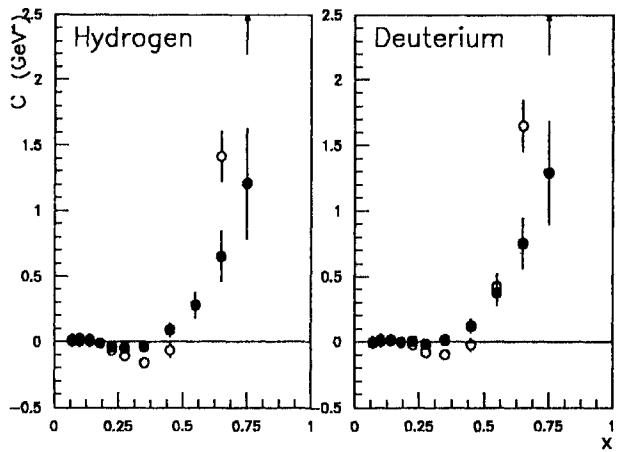


Figure 3: The higher-twist coefficients C_i as a function of x for H_2 and D_2 data. Full (open) circles are for fits with (without) TMC.

the fact that we have imposed that α_S show no Q^2 variation. In perturbative QCD, $\alpha_s(Q^2)$ is expected to decrease significantly from 1 to 250 GeV² (by a factor 2.5), and we want to see if the data are statistically powerful enough to favor the running of α_s . These " α_S = constant" fits have slightly worse χ^2 's, the difference with QCD fits being a bit over 10 units. The resulting higher-twist coefficients C_i , however, are significantly larger than in the QCD fits. This is illustrated in Figure 4 (analogous to Figure 1 bottomleft), where the amount of higher-twist terms needed to decribe the Q^2 -evolution of F_2 is indicated in each x bin by the difference between the solid and dashed lines. Obviously, it is much more natural to have a running α_S with very small higher-twist terms than a constant α_S and large higher-twist contributions. We consider that this comparison gives a strong physical indication for the running of α_s .

We have presented combined QCD fits to the two highest statistics F2 data on hydrogen and deuterium targets. These data are in good agreement and are complementary: the high Q2 data of BCDMS allow to test the perturbative QCD predictions and the low Q² data of SLAC lead to a precise determination of the magnitude of non-perturbative effects in the Q²evolution of F2. The data are well described over the whole Q^2 -range (0.5 to 250 GeV^2) by perturbative QCD fits including target mass corrections and higher-twist terms; these terms are very small or negligible at low x (x < 0.40) and they are small, positive and rise with x at higher x. The value of α_S obtained from these fits constitutes the most precise measurement of this fundamental quantity. Moreover, the data give an indication for the running of α_s .

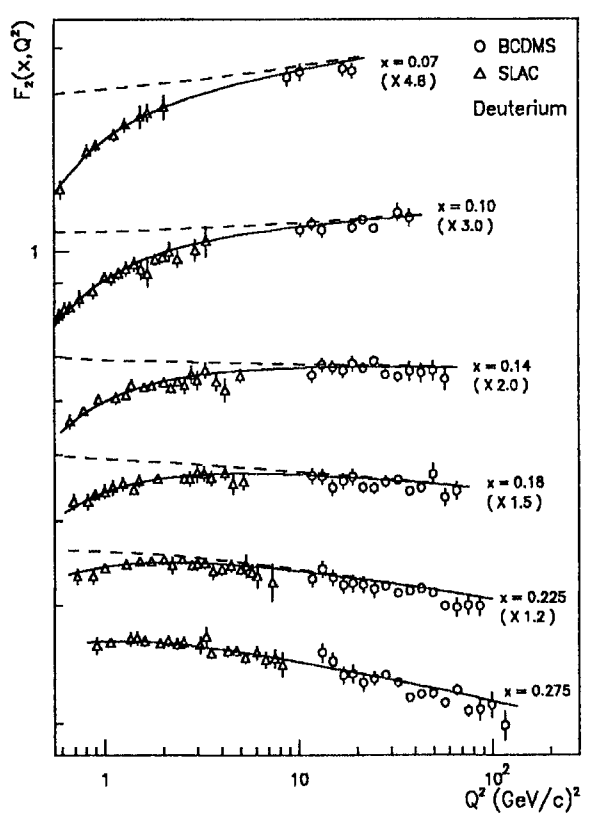


Figure 4: $\alpha_S = cst$ fit to the deuterium data for x < 0.30. The solid lines are the result of the fit and the dashed lines visualize the Q^2 evolution with no HT. This can be compared directly with Figure 1 (bottom-left).

The work presented here has been done in collaboration with A. Milsztajn, A. Staude, K.M. Teichert, M. Virchaux and R. Voss.

References

- BCDMS collaboration, A.C. Benvenuti et al.,
 Phys. Lett. 223B (1989) 485;
 BCDMS collaboration, A.C. Benvenuti et al.,
 Phys. Lett. 237B (1990) 592.
- [2] BCDMS collaboration, A.C. Benvenuti et al., Phys. Lett. 223B (1989) 490.
- [3] L. Whitlow, Ph D Thesis, SLAC-Report-357 (1990);
 A. Bodek, contribution to the workshop on parton distributions and structure functions, Fermilab, April 1990.
- [4] A. Milsztajn et al., preprint CERN-PPE/90-135.
- [5] The full data and error tables corresponding to [1] can be found in preprints CERN-EP/89-06 and CERN-EP/89-170.
- [6] M. Virchaux, Thèse, Université Paris-7 (1988);
 A. Ouraou, Thèse, Université Paris-11 (1988).
- [7] H. Georgi and D. Politzer, Phys. Rev. D14 (1976) 1829.
- [8] see e.g. F. Dydak, rapporteur talk at this conference.

Comparison of Structure Function Measurements from Hydrogen and Deuterium

T SLOAN University of Lancaster, UK

K BAZIZI and S J WIMPENNY University of California, Riverside, Ca, USA

ABSTRACT

Comparison of the measured structure functions for the proton and deuteron from the SLAC, BCDMS, NMC and EMC are made. A consistent set of structure functions from the four collaborations is obtained if small normalisation shifts are made to the data and the same theoretical model for $R = \sigma_L/\sigma_T$ is assumed to derive F_2 from each data set.

Over the past few years there have been many discussions of the apparent disagreements in the measurements of the proton structure function F_2 . Fig. 1 shows the data as published [1,2,3], which has been presented as evidence for disagreements between the experiments. We show below that if the F_2 values are derived with the same input theoretical model for $R = \sigma_L/\sigma_T$, reasonable consistency is obtained between the different data sets if small relative normalisation shifts within the quoted normalisation uncertainties are applied. Here σ_L and σ_T are the total cross sections for the absorption of longitudinal and transverse photons, respectively.

The values of F_2 in fig. 1 from each group have been obtained with different models for R. Since R is rather imprecisely measured, it is necessary to assume a model to calculate it in order to derive F_2 from the measured cross section which is a function of two unknown structure functions (in this case F_2 and R). BCDMS compute R from QCD, SLAC use values derived from their measurements which are similar to those computed from QCD and EMC take R=0, as expected from the quark parton model. Recent measurements of R [1] are in reasonable agreement with QCD calculations [4] when target mass corrections [5] are included. This model will be adopted here.

In this paper we rederive all the values of F_2 from the three groups using this same theoretical model to compute R for each group. In addition, the data are renormalised within their normalisation uncertainties which are taken to be approximately gaussian. The value of F_2 are insensitive to R for x > 0.1, but for x < 0.1 the differences are significant compared to the differences in fig. 1.

Fig. 2 shows the data in fig. 1 with F_2 rederived in this way for all three groups. Normalisa-

tion shifts of -2% are applied to the BCDMS data (quoted uncertainty 3%) and +7.5% to the EMC data (quoted uncertainty 5%). A much more consistent picture emerges with reasonable agreement between BCDMS and EMC at large Q^2 and fairly smooth extrapolation between the lower Q^2 SLAC data and the CERN data at larger Q^2 . Some minor disagreements remain in the overlap region between BCDMS and SLAC at large x. In addition the BCDMS data tend to lie below EMC in the largest x bin where the EMC errors are very large. It has been shown at this conference [6] that an increase of the BCDMS F_2 values by 1.5 times the quoted main systematic error brings the BCDMS and SLAC data into agreement in the overlap region at large x. Such an increase will also decrease any residual difference with the EMC data in this region.

Fig. 3 shows the slopes $dF_2/dln(Q^2)$ as a function of x for the BCDMS and EMC data compared to the predictions of QCD. There is good agreement between the data sets indicating that any angular dependent systematic shifts are under control. In addition, there is good agreement with the predictions of QCD.

Fig. 4 shows the ratio F_2n/F_2p as a function of x from the EMC[7], BCDMS[8] and NM-C[9]. Within the quoted errors there is good agreement between the three data sets. Since F_2n is related to the structure function for deuterium $(F_2n/F_2p \sim 2F_2d/F_2p - 1$, neglecting smearing effects), this implies that there is similar consistency between the deuterium data from EMC, BCDMS and SLAC to the proton data providing that the same normalisation corrections are made and the same assumptions for R are used to extract F_2 .

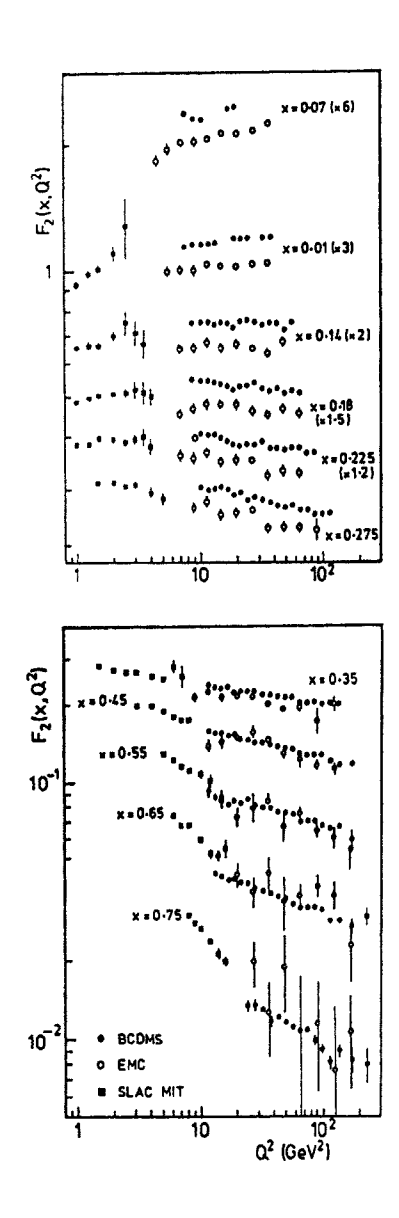


Fig. 1 The data on F_2 as published [1,2,3] using different models for R by each group and before any normalisation shift.

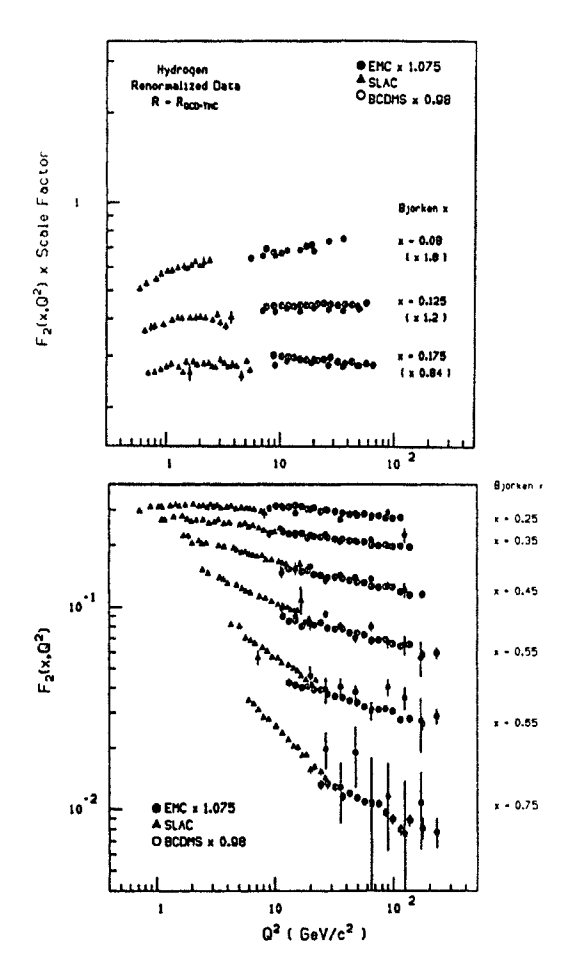


Fig. 2 The data from SLAC, EMC and BCDMS, using the same theoretical model for R to extract F_2 and with the small normalisation shifts indicated.

Conclusions

We find that a reasonably consistent picture of the proton and deuterium structure function measurements is obtained for the data from SLAC, BCDMS, EMC and NMC providing that the same assumed variation of R is assumed to extract F_2 and small relative normalisation shifts within the normalisation uncertainties are applied to the data.

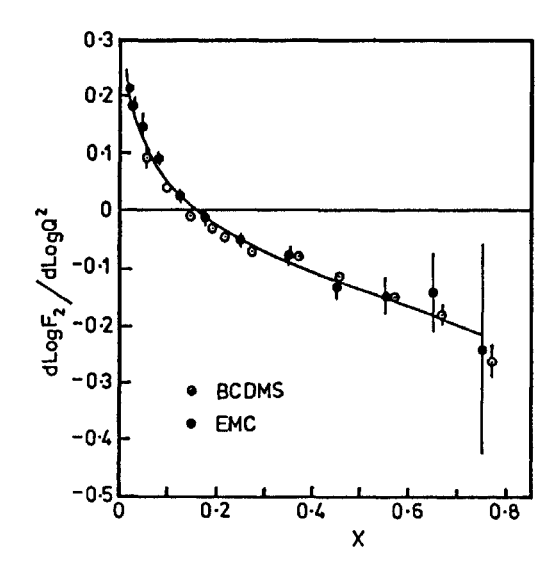


Fig. 3 The measured slopes $d \, \ell n F_2/d \, \ell n Q^2$ as a function of x. The smooth curve represents the behaviour expected from QCD with $\Lambda_{LO}=230$ MEV.

References

- 1. SLAC, L W Whitlow, PhD thesis, SLAC report 357 (1990) and references therein.
- BCDMS, A C Benvenuti et al, Phys. Lett. 223B (1989) 485.
- EMC, J J Aubert et al, Nucl. Phys. B259 (1985) 189.
- M Gluck and E Reya, Nucl. Phys. B145 (1978) 24.
 - G Altarelli and G Martinelli, Phys. Lett. 76B (1978) 89.
- H Georgi and D Politzer, Phys. Rev. **D14** (1976) 1829.
- 6. A Ouraou, These proceedings.
- EMC, J J Aubert et al, Nucl. Phys. B293 (1987) 740.
- 8. BCDMS, A C Benvenuti et al, *Phys. Lett.* 237B (1990) 592.
- 9. NMC, D Allasia et al, preprint CERN-PPE/90-103
- EMC, J Ashman et al, Nucl. Phys. B328 (1989) 1.

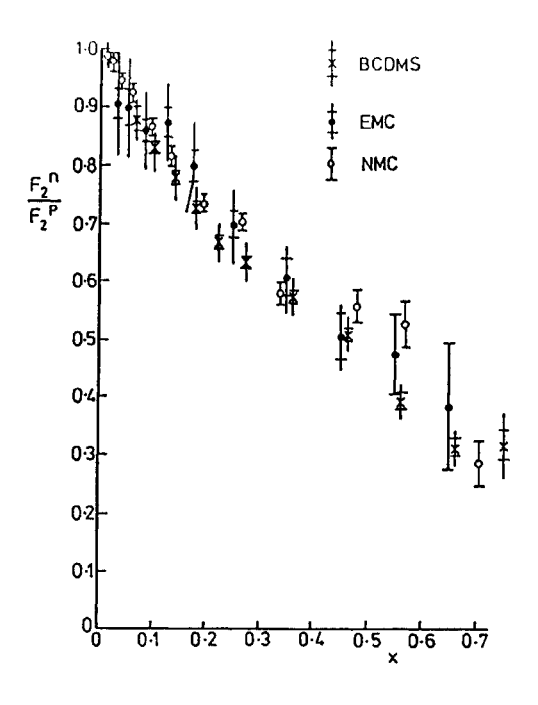


Fig. 4 Ratio F_2n/F_2p . Inner errors are statistical, outer systematic and statistical combined.

DISCUSSION

- Q. A. W. Thomas (Univ. Adelaide): Could you please clarify the effect of this analysis on the spin sum rule for the proton published by the EMC[10].
- A. T. Sloan: It will increase the value of the integral of the spin structure function g_1 by 3.2% of the value quoted in [10]. This integral is relatively insensitive to the changes in F_2 discussed here since the spin result (see table 9 of [10] was obtained by averaging over F_2 determined from several sources.

THE PROTON SPIN, THE AXIAL ANOMALY, THE U(1) PROBLEM AND ALL THAT

Jacques SOFFER

Centre de Physique Théorique, CNRS-Luminy, Case 907, 13288 Marseille cedex 9, France

ABSTRACT

Various aspects of the proton spin structure are discussed in particular, the present situation of the role played by the axial anomaly, the U(1) problem and the connection of the quark spins with the η '-meson coupling constants.

1. WHAT IS THE PROBLEM?

Let us recall that the proton spin problem arose with the new measurement performed by the European Muon Collaboration (EMC) of the proton spin-dependent structure function $g_1^p(x)$, down to the very small x-region [1]. The first moment of $g_1^p(x)$ was accurately determined and found to be

$$\Gamma_1^p = \int_0^1 dx g_1^p(x) = 0.126 \pm 0.010 \pm 0.015$$
 (1)

much smaller than anticipated [2]. The naive interpretation of this important result, combined with informations on hyperon β -decay, is that the total fraction of the proton spin carried by the quarks (and antiquarks)

$$\Delta \Sigma = \sum_{f} (\Delta q_f + \Delta \bar{q}_f)$$
 (2)

where $\Delta q_f = \int_0^1 dx \left(q_f^+(x) - q_f^-(x)\right)$ (and idem for \bar{q}) is compatible with zero, $\Delta \Sigma = (3 \pm 9 \pm 17)\%$. Usually $\Delta \Sigma$ is assumed to be related to the expectation value between proton states of the flavor singlet axial quark current $j_\mu^5 = \sum_f \bar{q}_f \gamma_\mu \gamma_5 q_f$. This small value of $\Delta \Sigma$ constrasts with the naive constituent quark model (NQM) where the proton is made of quarks in s-state, so that $\Delta \Sigma \simeq 1$. In ref. [2] it was explicitly assumed that for the strange quark $\Delta s = 0$, whereas $\Delta \Sigma \sim 0$ corresponds to Δs large and negative ($\Delta s \sim -\cdot 25$).

Several obvious questions must be asked and in particular: Is there something wrong with the proton spin? Why is the fraction of the proton spin carried by strange quarks so large? How do we understand Γ_1^p in perturbative QCD? Are there important non-perturbative effects? This situation has produced a vast theoretical debate and has generated a stream of papers. We will only discuss few of the very many current ideas and try clarifying some problems related to them.

2. THE AXIAL ANOMALY CONTRIBUTION

From the factorization theorem in perturbative QCD, it was proven [3] that the singlet part of Γ_1^p reads

$$\Gamma_1^{\text{singl.}} = \frac{\langle e_f^2 \rangle}{2} \left(\Delta \Sigma - N_f \frac{\alpha_s}{2\pi} \Delta g \right)$$
 (3)

where N_f is the number of quark flavor and $\langle e_f^2 \rangle$ is the average over the quark charges. The first term corresponds, for deep inelastic scattering, to the naive parton model (fig. 1a) whereas the second term is due to the short-range interaction of photons with polarized gluons via the quark box diagram (fig. 1b).

Indeed, photons see the gluon helicity distribution Δg , because of the axial anomaly resulting from the non-conservation of j_{μ}^{5} . This gluonic contribution need not to be a small correction because Δg grows with Q^{2} such that $\Delta g \sim \alpha_{s}^{-1}$, due to the evolution equations. Both $\Delta \Sigma$ and $\widetilde{\Delta g} = N_{f} \frac{\alpha_{s}}{2\pi} \Delta g$ are Q^{2} independent and the EMC result (eq. (1))

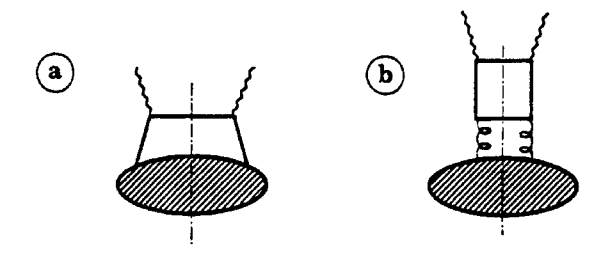


Fig. 1

which also reads

$$\Gamma_1^{\text{singl.}} = \frac{\langle e_f^2 \rangle}{2} (0.12 \pm 0.09 \pm 0.14)$$
(4)

can be interpreted as a compensation between $\Delta\Sigma$ and Δg . Of course this implies a large and positive gluon polarization $\Delta g \sim 5$. This approach has been strongly criticized [4,5] on the basis of the following arguments: i) the box contribution to $\Gamma_1^{\text{singl.}}$ has infrared instabilities, i.e. one gets different answers if the quark squared mass $m_q^2 = 0$ and the gluon squared mass $k^2 \neq 0$ or if vice versa $m_q^2 \neq 0$ and $k^2 = 0$, so this correction cannot be properly defined ii) there is only one operator, i.e. j^5_{μ} , which couples to $\Gamma_1^{\text{singl.}}$, so from the absence of a local gauge invariant gluon spin operator, it seems meaningless to try to separate gluon and quark contributions. These objections have been answered [6,7] and a direct calculation [8] of the box diagram for $m_q^2 \neq 0$ and $k^2 \neq 0$ in the scaling limit $Q^2 \rightarrow \infty$, shows that this contribution has two well defined gauge invariant local limits. One has

$$\Gamma_1^{\text{Box}} = -\frac{\alpha_s}{2\pi} N_f \left[1 + \frac{2\epsilon}{\sqrt{1+4\epsilon}} ln \frac{\sqrt{1+4\epsilon}-1}{\sqrt{1+4\epsilon}+1} \right]$$
 (5)

where $\epsilon = m_q^2/k^2$ and one finds

$$\Gamma_1^{\text{Box}} \longrightarrow \begin{cases}
-\frac{\alpha_s}{2\pi} N_f & \text{for } \epsilon \to 0 \\
0 & \text{for } \epsilon^{-1} \to 0
\end{cases}$$
 (6)

These two limits correspond to two different definitions of $\Delta\Sigma$ and different evolution equations.

In the first case,

$$\Delta \dot{\Sigma} = 0 \text{ and } \Delta \dot{\Sigma} - \dot{\widetilde{\Delta g}} = \gamma (\Delta \Sigma - \widetilde{\Delta g})$$
 (7)

(. means $d/dlnQ^2$ and $\gamma = -\alpha_s^2/2\pi^2N_f$) so $\Delta\Sigma$ is conserved and the anomaly is included in the subprocess. In the second case, the anomaly is

in the quark distribution and with $\Delta \Sigma' = \Delta \Sigma - \widetilde{\Delta g}$ we have

$$\Delta \dot{\Sigma}' = \gamma \Delta \Sigma' \text{ and } \Delta \dot{\Sigma}' + \dot{\widetilde{\Delta g}} = 0$$
 (8)

The first solution is more natural for light quarks because eqs. (7) are just the analytic continuation of the evolution equations for higher moments $m \geq 2$ and it is not ambiguous if the quark term is specified as a conserved quantity.

Concerning gauge invariance, the problem does not arise for $m \geq 2$ because one can built from the quark fields q_f and the gluon fields A^a_{ν} , two local for gauge invariant operators. Therefore $\Delta \Sigma$ and $\widetilde{\Delta g}$ can be defined as analytic continuation to m=1 of gauge invariant quantities. In the axial gauge $n_{\nu}A_{\nu}=0$ one has

$$\Delta \Sigma = \frac{1}{2} \langle p | j_{\nu}^5 - K_{\nu} | p \rangle n_{\nu} \text{ and } \widetilde{\Delta g} = -\frac{1}{2} \langle p | K_{\nu} | p \rangle n_{\nu}$$
(9)

where j_{ν}^{5} introduced before is the quark spin operator and $K_{\nu} = N_{f} \frac{\alpha_{\star}}{2\pi} \epsilon_{\nu\mu\sigma\rho} A_{\mu}^{a} F_{\sigma\rho}^{a}$ is the gluon spin operator. The substraction of the anomaly makes $\Delta\Sigma Q^{2}$ -independent as a consequence of the Adler-Bardeen relation

$$\partial_{\nu}j_{\nu}^{5} = \partial_{\nu}K_{\nu} = N_{f}\frac{\alpha_{s}}{2\pi}F_{\rho\sigma}^{a}\widetilde{F}_{\rho\sigma}^{a} \equiv Q \qquad (10)$$

The non-gauge invariance of K_{ν} is connected to a term non-analytic in m due to a non-perturbative contribution [9] and although K_{ν} is not the gluon spin, its projection $K_{\nu}n_{\nu}$ is invariant under infinitesimal gauge transformations of perturbative QCD.

3. THE RELATION TO THE U(1) PROBLEM

For non-symmetric matrix elements of these currents j_{ν}^{5} and K_{ν} , in any covariant gauge, one has

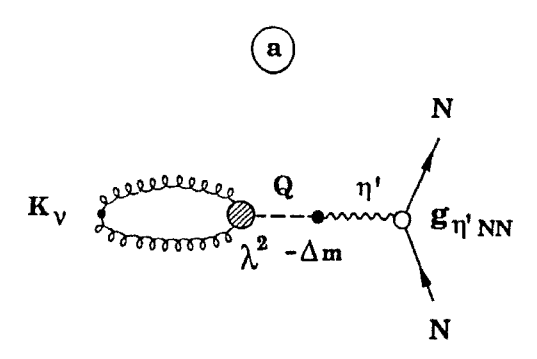
$$\langle p'|j_{\nu}^{5}|p\rangle = \bar{u}(p') \left[\gamma_{\nu} G_{1}(q^{2}) + q_{\nu} G_{2}(q^{2}) \right] \gamma_{5} u(p) \langle p'|K_{\nu}|p\rangle = \bar{u}(p') \left[\gamma_{\nu} \widetilde{G}_{1}(q^{2}) + q_{\nu} \widetilde{G}_{2}(q^{2}) \right] \gamma_{5} u(p)$$
(11)

From the gauge invariance of $\partial_{\nu}K_{\nu}$ and in the absence of a zero mass axial pole in perturbative QCD i.e.

$$\lim_{q^2 \to 0} q^2 G_2(q^2) = \lim_{q^2 \to 0} q^2 \widetilde{G}_2(q^2) = 0$$
 (12)

one has $G_1(0) = \Delta \Sigma - \widetilde{\Delta g}$ and $\widetilde{G}_1(0) = -\widetilde{\Delta g}$ which

are two quantities manifestly gauge invariant. However this is not true in general because for the resolution of the U(1) problem in QCD, K_{ν} must couple to a zero mass ghost pole whose mixing with the ninth Nambu-Goldstone boson η'_0 , gives an additional mass $\Delta m_{\eta'} = \lambda^2/f_{\eta'}$ where λ^2 characterizes the ghost coupling and $f_{\eta'}$ is the η' decay constant. The ghost contributions are shown in figs. (2a,b), where we consider the possibilities of a coupling of the ghost to $\bar{N}N$ either through the physical η' or directly.



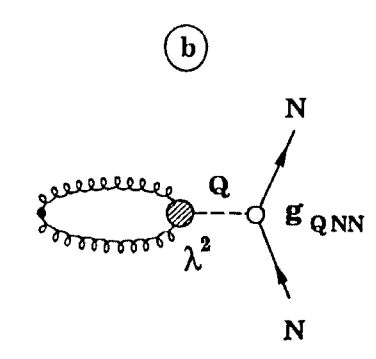


Fig. 2

In this case eq. (12) does not hold since we have

$$q^2 \widetilde{G}_2(q^2) = \sqrt{N_f} \lambda^2 \left(\frac{\Delta m_{\eta'} g_{\eta'NN}}{\Delta m_{\eta'}^2 - q^2} - g_{QNN} \right)$$
(13)

Now using eq. (11) and the Adler-Bardeen relation one gets

$$2M\left(G_{1}(q^{2})-\widetilde{G}_{1}(q^{2})\right)=q^{2}\left(G_{2}(q^{2})-\widetilde{G}_{2}(q^{2})\right) \tag{14}$$

both sides being renormalization group invariant because of the conservation of $j_{\nu}^{5} - K_{\nu}$. So in the limit $q^{2} \rightarrow 0$ one obtains [11]

$$\Delta \Sigma = \frac{N_f f_{\eta'} g_{\eta'_0 NN}}{2M} \tag{15}$$

where $g_{\eta'_0NN} = g_{\eta'NN} - \Delta m_{\eta'}g_Q$ is the η'_0 coupling constant to $\bar{N}N$.

One gets a different result in an approach which uses an effective chiral Lagrangian [12], where $\widetilde{G}_1(0)$ is disregarded. As a consequence, the EMC result is interpreted as the vanishing of $g_{\eta'_0NN}$. We believe that presumably g_{QNN} is small, so if one assumes $g_{\eta'_0NN} \simeq g_{\eta'NN} \simeq 7.5$ (in reasonable agreement with SU(6) i.e. $g_{\eta'NN} = g_{\pi NN} \sqrt{6}/5 = 6.8$), eq. (15) yields $\Delta\Sigma \simeq 1.14$ which is remarkably close to the NQM value!

Very recently the corrections to eq. (15) due to quark masses and to $\eta - \eta' - \pi^{\circ}$ mixing have been calculated [13]. We recall that two large corrections due to the π° admixture and to the light quark masses u and d, which have opposite signs for proton and neutron, cancel out exactly and therefore one does not observe isospin violations. The final result is

$$\Delta \Sigma = \frac{\sqrt{N}_f}{2M} f_{\eta'} \Delta m_{\eta'}^2 \left[\frac{g_{\eta'NN}}{m_{\eta'}^2} \cos\theta_3 - \frac{g_{\eta NN}}{m_{\eta}^2} \sin\theta_3 \right] - \frac{1}{2} g_A^s \quad (15')$$

whose numerical value is 0.94!

4. WHAT IS NEXT?

Clearly one needs a further confirmation of the EMC result on $g_1^p(x)$ and also a measurement of $g_1^n(x)$ on neutron. Whereas the Ellis-Jaffe sum rule [2] is modified by Δg , this is not the case for the Bjorken sum rule [14]

$$\int_{0}^{1} \left(g_{1}^{p}(x) - g_{1}^{n}(x) \right) dx = \frac{1}{6} g_{A} \left(1 - \frac{\alpha_{s}}{\pi} \right)$$
 (16)

which is protected from the anomaly and has a small QCD correction. It could be wrong [15] and this burning question largely justifies several proposals for making this crucial experiment at CERN (NMC collaboration) and at HERA (HERMES collaboration). We also recall that there is a strong phenomenological argument based on positivity [16], against a large measured Δs , which gives

$$|\Delta s| \langle 0.052 +0.023 \atop -0.053$$
 (17)

From ref. [8] it was also found that $\Delta g(x)$ is small at finite Q^2 and contributes only in the very small x-region, below the EMC data. However due to the regularization procedure, there are some ambiguities in the short range contribution of the triangle diagram which lead to an ambiguity in the quark contribution and could also modify the evolution equations.

One should hunt for direct evidence of a large and positive Δg , for example, in polarized pp collisions (direct photon, jet production, etc...) and one should also try to get a better determination of $g_{\eta'NN}$. To conclude, the proton spin problem is more challenging than ever!

REFERENCES

- J. Ashman et al. (EMC), Nucl. Phys. B328 (1989) 1.
- J. Ellis and R. Jaffe, Phys. Rev. D9 (1974) 1444.
- 3. A.V. Efremov and O.V. Teryaev, Preprint Dubna, JINR, E2-88-287 (1988).
 - G. Altarelli and G.G. Ross, *Phys. Lett.* **B212** (1988) 381.
 - R.D. Carlitz, J.C. Collins and A.H. Mueller, *Phys. Lett.* **B214** (1988) 229.
- R.L. Jaffe and A. Manohar, Nucl. Phys. B337 (1990) 509.
- G. Bodwin and J. Qiu, Phys. Rev. **D41** (1990) 2755.
- A.V. Efremov, J. Soffer and O.V. Teryaev, Nucl. Phys. B346 (1990) 97.
- G. Altarelli and B. Lampe, Z. Phys. C47 (1990) 315.

- S.D. Bass, N.N. Nikolaev and A.W. Thomas, Adelaide University preprint ADP-133-T80 (1990).
- S. Forte, Phys. Lett. B224 (1989) 189;
 Nucl. Phys. B331 (1990) 1.
- 10. G. Veneziano, Nucl. Phys. B159 (1979) 213.
- A.V. Efremov, J. Soffer and N. Törnqvist, *Phys. Rev. Lett.* **64** (1990) 1495.
- G. Veneziano, Mod. Phys. Lett. A4 (1989) 1605.
 - G.M. Shore and G. Veneziano, *Phys. Lett.* **B244** (1990) 75.
- A.V. Efremov, J. Soffer and N. Törnqvist, Preprint Marseille CPT-90/P.2402.
- 14. J.D. Bjorken, Phys. Rev. D1 (1970) 1976.
- G. Preparata, Ph. Ratcliffe and J. Soffer, Phys. Lett. B231 (1989) 483.
- 16. G. Preparata and J. Soffer, Phys. Rev. Lett.
 61 (1988) 1167; Erratum Phys. Rev. Lett.
 62 (1989) 123.

DISCUSSION

- Q. A. Kisselev (IHEP, Protvino): There is a serious inconsistency of your main result. The point is that gluon contribution s_g does depend on large gauge transformation. So, according to your definition of quark contribution to the proton spin Σ , it must also depend on a gauge chosen. That is why Σ cannot be directly related with hadron couplings, which are physical gauge independent quantities.
- A. J. Soffer: I work at the perturbative level. And in perturbative QCD gluon contribution to the proton spin s_g remains invariant under relevant gauge transformation.

On the Proton Spin Content

B.L.Ioffe Inst. of Theoretical and Experimental Physics, 117259 Moscow, USSR

and

M.Karliner School of Physics & Astronomy, Tel-Aviv Univ.,69978 Tel-Aviv, Israel

Abstract

Experimental data suggest that strange quarks in the proton carry a small part of the proton momentum, but a relatively large part of the spin projection. To resolve this problem a hypothesis is conjectured that the appearance of ss pairs in the proton is caused by the same nonperturbative mechanism (instantons) which probably is responsible for Okubo-Zweig-Iizuka rule violation in mesons. The experiments in which this hypothesis can be tested are proposed.

I.Introduction.

The recent experimental results of EMC [1] on deep inelastic scattering of polarized muons on polarized protons (together with the earlier results of SLAC [2]) indicate [1,3,4] that a large part of the proton spin projection is carried by strange quarks. The description of the data gives [1,3,4]

$$\Delta s = \int_{0}^{1} dx [s_{+}(x) - s_{-}(x)] \simeq -0.20$$
 (1)

where $s_{+-}(x)$ are s-quark distributions with helicities 1/2. As follows from the same data Δu =0.78, Δd =-0.47. Therefore Δs is comparable with the part of the proton spin projection carried by u- and d- quarks. Since $\Delta q^{\sim} \langle p | \bar{q} \gamma_{\mu} \gamma_5 q | p \rangle$ q=u, d, s the EMC result indicate a relatively large matrix element in the proton of the operator $\bar{s} \gamma_{\mu} \gamma_5 s$. On the other hand, it is known experimentally [5] that the part of the proton momentum carried by strange quarks is small

$$V_2^S = \int_0^1 [s_+(x) + s_-(x)] x dx = 0.026 \pm 0.006$$
 (2)

 V_2^S is proportional to the matrix element $\langle p | \theta_{\mu\nu}^S | p \rangle$, where $\theta_{\mu\nu}^S$ is the energy-momentum tensor of strange quarks.

The question arise: how these two facts can be reconsiled? We propose a possible solution of this problem. We point out that the question 'how many strange quark pairs are there in the proton?' is not well defined until one specifies the operator which is discussed. A similar situation is well known in mesons. The question of strange quark content, or the degree to which the Okubo-Zweig-Iizuka (OZI) rule

works strongly depends on the spin and parity of the mesons: in vector and tensor nonets the mixture of ss and uu+dd is very small, while in pseudoscalar nonet it is of the order O(1). These facts cannot be explained by perturbative QCD.

2. Instantons and Quark Mixing.

The qualitative explanation of the OZI rule realization and violation in meson multiplets was proposed in Ref.6. It was suggested that the most important nonperturbative configurations of the gluonic field in QCD vacuum are of the instanton type. Consider the mixed polarization operator, representing OZI rule violation:

II^{S,u+d}(x,y)=<0|T{j^S(x),j^{u+d}(y)}|0> (3) where j^{S,u,d} are V,A,P,S,T currents of s,u,d quarks.Disregard the perturbative gluon exchange and take quarks as moving in an external instanton field. Then the r.h.s.of eq.(3) factorizes (Fig.1)

$$\Pi^{s,u+d}(x,y) = \langle 0 | j^{s}(x) | 0 \rangle_{inst}^{\times}$$

$$\langle 0 | j^{u+d}(y) | 0 \rangle_{inst} \bar{u}(d)$$

$$\downarrow s$$

Fig.1 The diagram representing the mixed polarization operator (4) in the instanton field. The instanton is depicted by the black point.

It was shown in Ref.6 that the matrix elements $\langle 0|j(x)|0\rangle_{inst}$ in the delute instanton gas approximation are zero

for V and T currents and nonvanishing for A,P and S currents. The saturation of the polarization operator (3) by the contributions of meson states results in qualitative explanation of the OZI rule in meson multiplets.

A characteristic feature of the proposed nonperturbative mechanism is the strong momentum dependence of Π^s , which arises from exponential α_s dependence of nonperturbative effects "exp(-2 π/α_s). This property is very desirable: it explains the disappearance of nonperturbative cc and qq mixing in the charmonium region.

We assume that the same nonperturbative mechanism is responsible for ss and uu+dd mixing in the proton (Fig.2).

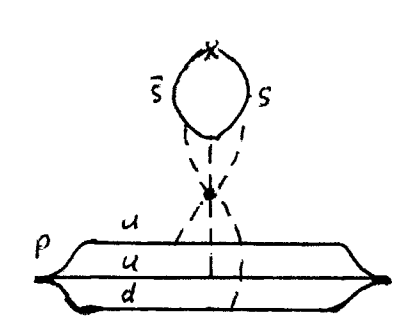


Fig.2 A direct consequence of this hypothesis is that $\langle p\,|\,\theta^S_{\mu\nu}|\,p\rangle$ does not receive

contributions from nonperturbative effects. Therefore the part of the proton momentum carried by strange quarks ought to be small if one adopt the common belief that perturbative effects are small even at 1 GeV.

In the framework of our hypothesis $\langle p | \bar{s} \gamma_{\mu} \gamma_5 s | p \rangle \neq 0$ due to nonperturbative mechanism described by the diagram of Fig.2. At momentum transfer $q_{\mu} \neq 0$ the matrix element $\langle p | \bar{s} \gamma_{\mu} \gamma_5 s | p \rangle$ is proportional to s-quark contribution to the proton axial formfactor $G_A^S(Q^2), Q^2 = -q^2$. At $Q^2 \geqslant 1$ GeV² $G_A^S(Q^2)$ decreases very steepely with Q^2 increasing, $G_A^S(Q^2)^{\sim}$ $(1/Q^{2n})$, $n \geqslant 5$. The large Q^2 behaviour of the formfactor is connected with $x \Rightarrow 1$ behaviour of the corresponding structure functions through the Drell-Yan relation: $(1/Q^2)^n \Rightarrow (1-x)^p$, p = 2n-1. We expect at $x \Rightarrow 1$ s₊ $(x) - s_-(x)^{\sim}(1-x)^p$, $p \geqslant 10$. At small $x s_+ - s_-$ is dominated by the

a₁ exchange, the intercept of the a₁ trajectory being close to zero. Therefore we propose the parametrization

$$s_{\perp}(x)-s_{-}(x)=B(1-x)^{p}$$
 (5)

The sum $s_+ + s_-$ can be parametrized as

$$s_+(x)+s_-(x)=(A/x)(1-x)^k+C(x)$$
 (6)
In the first term in the r.h.s. of (6)
the 1/x factor comes from the pomeron
exchange at small x, the factor $(1-x)^k$
 $k\approx 5$ corresponds to quark counting rule
at x=1 (see e.g.[7]). The term $C(x)$
represents the nonperturbative contri-
bution to s_++s_- . According to our hypo-
thesis

$$\int_{0}^{1} x C(x) dx = 0 \tag{7}$$

It can be shown that unlike the situation [8], where s_+-s_- and s_++s_- have approximately the same behaviour at $x\Rightarrow 1$, in our case the positivity requirement of $s_+(x)$ and $s_-(x)$ is not in contradiction with large Δs and small V_2 . Let as temporarely ignore C(x) in (6). From the positivity requirement of $s_+(x)$ and $s_-(x)$ it follows that

 $|\Delta s| \leqslant V_2^s \frac{(k+1)(p-k+1)^{p-k+1}}{(p+1)(p-k)^{p-k}} \tag{8}$ The inequality (8) is not restrictive at large p: for p=10 and k=5 $|\Delta s| \leqslant 8V_2^s$ and there is no contradiction between $\Delta s \simeq -0.20$ and V_2^s in (2).

We expect that at x=1 C(x) has approximately the same behaviour as (5): $C(x)^{\alpha}(1-x)^{p'}$, p'=p and at x<0.1 can be comparable with the first term in r.h.s. of (6). Evidently, inclusion of C(x) into (6) does not qualitatively change the inequality (8). For distribution of light antiquarks q=u,d we have $C_{\overline{q}}(x) \simeq C_{s}(x)$. But sinse the ratio of momenta carried by strange and q sea is about 0.4, the nonperturbative component is relatively more important in the strange sea, than in q sea.

Experimental Consequences.

A direct experimental test of our hypothesis can be carried out by measuring strange particle production in polarized $\mu(e)$ scattering on the polarized proton. We expect that the most of the events in such experiment will correspond to x \leq 0.1, s_+ - s_- "(1-x) p , p \approx 10

at large x.

Another possibility is the observation of nonperturbative component C(x) in $s_+ + s_-$, eq.(6). The CCFR collaboration data [10] on charm production in neutrino experiment in which s=s_+s_ distribution was measured give an indication in the favour of our hypothesis. The authors parametrize the sea distributions by $xs(x)=a_s(1-x)^{\alpha}$, $x\bar{q}(x)=a_{q}(1-x)^{\beta}$ and find $\alpha=10.8,\beta=6.9$. We can fit the data [10] using the parametrization (6) with

 $C(x)=(C/x)(1-bx)(1-x)^{p}, p'=p=12, k=5$ (9)

the same for s and q sea. (The factor 1-bx is introduced such that eq.(7) will be fulfilled.) The third possibility is the measurements of the axial formfactor in elastic ν_{p} scattering. We expect in this formfactor two structures: the usual one, which must concide [11] with the vector formfactor at large Q², and the nonperturbative one, fastly decreasing with Q². Therefore, in the axial formfactor, unlike the vector formfactor, where the dipole fit gives a good de-scription up to Q²≥10 GeV², we expect the deviation from the dipole fit at $Q^{2}\sim 1-2$ GeV².

Acknowledgements

We are grateful to S.Brodsky, M.Chanowitz, Y.Frishman and L.Susskind for fruitful discussions.

References

- 1.J.Ashman et al., *Phys. Lett.* **B206** (1988)364; *Nucl. Phys.* **B328** (1989)1.
 2.G.Baum et al., *Phys. Rev. Lett.* 45 (1980)2000, **51**(1983)1135.
 3.J.Ellis, *R.*Flores and S.Ritz, *Phys.*
- Lett. B198(1987)393.
- 4.S.Brodsky, J.Ellis and M.Karliner, Phys. Lett. B206(1988)309.
- 5.H.Abramowitz et al., Z.Phys. C15 (1982)19.
- $6. exttt{B.V.Geshkenbein}$ and $exttt{B.L.Ioffe}$, $exttt{Nucl.}$ Phys. **B166**(1980)340.
- 7.B.L. Toffe, V.A. Khoze and L.N. Lipatov, Hard Processes, Vol.1 (North Holland,
- Amsterdam, 1984), p.244. 8.G. Preparata and J Soffer, Phys. Rev.
- Lett. 61 (1988) 1167. E.Oltman, in The Storrs Meeting: 9.E.01tman, Proc. of the Division of Particles and Fields of APS, 1989, ed.K. Holler (World Scientific, Singapore, 1989).

10.C. Foundas et al., Phys. Rev. Lett. 64 (1990)1207.11.B.L.Ioffe, Phys. Lett. **B63**(1976)425.

A.W. THOMAS

Department of Physics and Mathematical Physics University of Adelaide, PO Box 498 Adelaide, S.A. 5001, AUSTRALIA.

and

A.W. SCHREIBER NIKHEF-K, P.O. Box 41882 1009 DB Amsterdam, THE NETHERLANDS.

and

A.I. SIGNAL

Department of Physics and Biophysics Massey University, Palmerston North, NEW ZEALAND.

There has recently been considerable progress in relating the spin-dependent parton momentum distributions measured in deep-inelastic scattering to familiar, low-energy quark models. We report predictions for the valence quark distribution and the polarisation asymmetry predicted by the MIT bag model. Some remarks are also made concerning the effect of restoring chiral symmetry by including the pion cloud of the nucleon. This is particularly relevant to the recently measured defect in the Gottfried sum-rule.

One of the outstanding successes of perturbative QCD (PQCD) is its ability to describe the variation of the quark and gluon distribution functions measured in deep inelastic scattering (DIS) over a wide range of momentum transfer. There has been much less progress on the non-perturbative problem of predicting these distributions at any one scale. Rather than tackling this directly, we shall examine the relationship between the DIS distribution functions and the quark models which have been so successful in describing low-energy hadronic properties. We concentrate particularly on the MIT bag model [1] including one gluon exchange and pionic corrections [2].

At a momentum scale (μ^2) appropriate to the model the twist-two quark distribution may be written as [3]

$$q(x) = p^{+}\sum_{n} \delta(p^{+}[1-x]-p_{n}^{+})|\langle n|\Psi+(0)|p,s\rangle|^{2}.$$
(1)

Here p⁺ is the plus component of the nucleon's momentum p, p_n ⁺ is the plus component of the intermediate state, $\hat{\Psi}_+$ is the quark field operator times $(1+\alpha_3)/2$, $|p,s\rangle$ refers to the initial nucleon state with

spin s and $\langle n|$ is the (colored) intermediate state.

It is common to absorb the delta function in equ.(1) into the matrix element in order to be able to perform the sum over intermediate states and hence obtain the quark distribution in terms of a matrix element corresponding to forward scattering. We shall not do this however because equ.(1) has a very useful property. Because both p^{+} and $p_{n}^{\,+}$ are positive the delta function ensures vanishing support for $x\,>\,1$, independent of the approximations that one invariably has to make for the states.

For the wavefunctions of the initial and intermediate states we use products of MIT bag wavefunctions $\Psi,$ with the centre of mass motion projected out by the use of the Peierls-Yoccoz procedure

$$\langle \mathbf{x}_1 \mathbf{x}_2 \mathbf{x}_3 | \mathbf{p}, \mathbf{s} \rangle = \frac{1}{\phi_3(\mathbf{p})} \int d\mathbf{R} e^{i \underline{\mathbf{p}} \cdot \underline{\mathbf{R}}} \prod_{i}^{3} \Psi(\mathbf{x}_i - \mathbf{R}).$$
 (2)

Here $\phi_3(p)$ ensures the normalization of the wavefunction and \underline{R} is the position of the centre of the bag. We obtain, for a quark of flavour f in a proton at rest,

$$q_{\rm f}^{\uparrow\downarrow}({\rm x}) \; = \; \frac{M}{(2\pi)^3} \; {\scriptstyle \sum \atop m} \langle \mu \, | \, P_{m,f} \, | \, \mu \rangle \; \; . \label{eq:qfi}$$

$$\int d \underline{p}_n \; \frac{ |\phi_2(\underline{p}_n)|^2}{|\phi_3(0)|^2} \; \delta(\underline{M[1-x]-p_n^+}) \, |\widetilde{\Psi}_{+,\,m}(\underline{p}_n)|^2 \; .$$

Here $P_{m,f}$ projects the states with spin mand flavor f out of wavefunction $|\mu\rangle$, m is the projection of the quark's spin in the direction of the proton spin and $\widetilde{\Psi}_{+,\,\mathrm{m}}$ is the (plus component of the) Fourier transform of the single quark wave-function with spin Not shown in equ.(3) are projection m. contributions, which we include, from processes where the photon probe produces a These are associated quark-antiquark pair. with intermediate states $|n\rangle$ in equ.(1) with either $3q-\overline{q}$ or 4q.

It is simple to phenomenologically incorporate the effects of one gluon exchange into equ.(3). One gluon exchange tends to increase (decrease) the mass of the intermediate diquark state, and thus effect p_n^+ , depending on whether it is in its spin triplet (singlet) state [4]. If we assume that the N- Δ mass splitting is due to one gluon exchange we find $(M_2^{triplet}-M_2^{singlet}) \sim 200 \text{MeV}$.

This completes the description of our model. Further details may be found in [5] and [6]. We shall fix the bag radius and the absolute scale of the diquark masses $\rm M_2^0$ (the splitting will be 200 MeV) by fitting the predictions, after QCD evolution, to the valence distribution at 10 $\rm \,GeV^2$ (Fig.1; we assume $\rm \Lambda_{\rm QCD}$ to be 200 MeV). This enables us

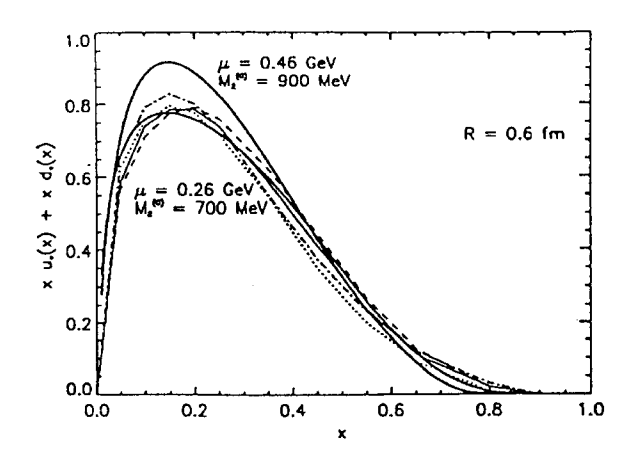


Figure 1: The valence distribution at $Q^2 = 10~\text{GeV}^2$ for two different sets of μ and $M_2^{(0)}$. The four thin curves are parameterizations of data taken from [7].

to fix the scale μ at which the model applies. We may then make predictions for other distributions at any scale Q^2 . The results for g_1^p at $10~{\rm GeV}^2$ are shown in Fig. 2, while predictions for g_1^n have been reported elsewhere [4,9].

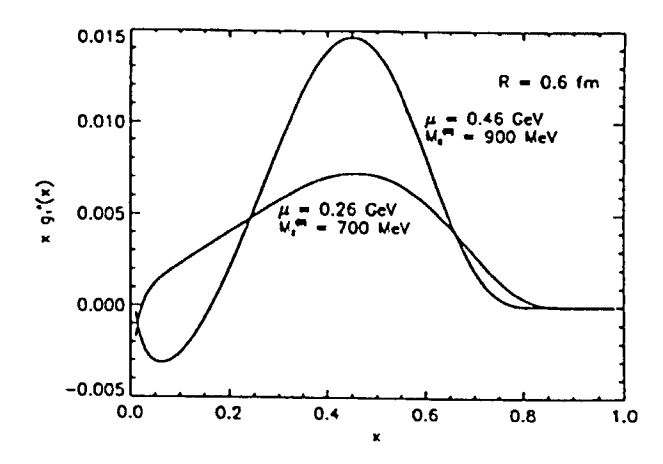


Figure 2: $g_1^p(x)$ at $Q^2 = 10 \text{ GeV}^2$ corresponding to the parameters in Fig. 1. The data is taken from [8].

Clearly the model leads to quite a good fit to the valence distribution, provided the bag scale μ is quite low - probably too low for evolution through leading order PQCD to be reliable. In this regard the restoration of chiral symmetry through adding a pion cloud to the bag is very important. The cloud of virtual pions takes momentum from the valence quarks so that it is not necessary to evolve so far to match data. Indeed, after allowing for this pion cloud one obtains a fit to xF3 as good as that shown in Fig. 1, but with μ^2 as high as 0.5 GeV².

The restoration of chiral symmetry has another consequence which is very significant in the light of a recent report that the Gottfried sum-rule is violated by some 30% [10]. To derive this sum-rule requires that the sea is SU(2) flavor symmetric, that is retains no knowledge of the flavor of the valence quarks. On the other hand, it has long been realized that the dominant, longrange pion emission pro- cess $p \rightarrow \pi^+ n$ implies $\overline{a} > \overline{u}$ [11]. This is countered a little by the N $\rightarrow \Delta \pi$ process, while the n=4 contribution to the sea of the bag (mentioned below equ.(3)) also implies $\overline{d} > \overline{u}$ because of the Pauli exclusion principle [5]. Overall it is quite possible to reproduce the observed sum rule for $(F_2^p - F_2^n)$ within the usual

range of pion coupling and bag parameters [12].

ACKNOWLEDGEMENTS

This work was supported in part by the Australian Research Council.

REFERENCES

- A. Chodos et al., Phys. Rev. **D10** (1974) 2599.
- A.W. Thomas, Adv. Nucl. Phys. 13 (1984)
 1.
- 3. R.L. Jaffe, Nucl. Phys. B229 (1983) 205.
- 4. F.E. Close and A.W. Thomas, *Phys. Lett.* 212B (1988) 227.
- A.I. Signal and A.W. Thomas, Phys. Rev. D40 (1989) 2832.
- 6. A.W. Schreiber, A.I. Signal and A.W. Thomas, to be published.
- 7. K. Charcula et al., preprint ZEUS 89-121 (1989).
- 8. EMC Collaboration, CERN-EP/89-73 (1989).
- 9. A.W. Schreiber, A.W. Thomas and J.T. Londergan, *Phys. Rev.* D (1990) to appear.
- 10. A.C. Benvenuti et al., Phys. Lett. 237B (1990) 592,599.
- 11. M. Ericson and A.W. Thomas, Phys. Lett.
 148B (1984) 191.
- 12. A.I. Signal, A.W. Schreiber and A.W. Thomas, Adelaide preprint, ADP-90-145/T89.